University of Essex — Essex Business School

Essex Finance Centre

Working Paper Series

Working Paper No 93: 12-2025

"An Unobserved Components Based Test for Asset Price Bubbles"

"Sam Astill, David I. Harvey, Stephen J. Leybourne and A. M. Robert Taylor"

Essex Business School, University of Essex, Wivenhoe Park, Colchester, CO4 3SQ
Web site: http://www.essex.ac.uk/ebs/

An Unobserved Components Based Test for Asset Price Bubbles*

Sam Astill[a], David I. Harvey[b], Stephen J. Leybourne[b] and A.M. Robert Taylor[a]

[a] Essex Business School, University of Essex

[b] Granger Centre for Time Series Econometrics and School of Economics, University of Nottingham

November 28, 2025

Abstract

The general solution of the standard stock pricing equation commonly employed in the finance literature decomposes the price of an asset into the sum of a fundamental price and a bubble component that is explosive in expectation. Despite this, the extant literature on bubble detection focuses almost exclusively on modelling asset prices using a single time-varying autoregressive process, a model which is not consistent with the general solution of the stock pricing equation. We consider a different approach, based on an unobserved components time series model whose components correspond to the fundamental and bubble parts of the general solution. Based on the locally best invariant testing principle, we derive a statistic for testing the null hypothesis that no bubble component is present, against the alternative that a bubble episode occurs in a given subsample of the data. In order to take an ambivalent stance on the possible number and timing of the bubble episodes, our proposed test is based on the maximum of a doubly recursive implementation of this statistic over all possible break dates. Simulation results show that our proposed tests can be significantly more powerful than the industry standard tests developed by Phillips, Shi and Yu (2015).

Keywords: rational bubbles; unobserved components model; locally best invariant testing principle; double recursion.

JEL Classification: C22; C12; G14.

*We are grateful to participants at the opening conference of the Aarhus Center for Econometrics, May 2025, for helpful comments. Address correspondence to: Robert Taylor, Essex Business School, University of Essex, Wivenhoe Park, Colchester, CO4 3SQ, UK. Email: robert.taylor@essex.ac.uk.

1 Introduction and Motivation

Asset price bubbles, defined as a large upward price swing additional to the fundamental price of the asset, represent a misallocation of resources during the upwards bubble phase and a potentially catastrophic loss of value during the (inevitable) crash phase. Where bubbles exist in assets or indices with large market capitalisations, crashes often lead to recessions due to deleveraging, combined with a loss of investor confidence, with significant ramifications for the real economy. Well known recent examples include the recessions in the early 2000s in the European Union and the USA following the collapse of the dotcom bubble, and the Global Financial Crisis of 2007/2008 following the excessive risk-taking of investors in the preceding years, in particular in the credit sector.

In the aftermath of the Global Financial Crisis, the detection of asset price bubbles has become an important element of macroprudential study and the econometric literature in this area has accordingly burgeoned. In particular, Phillips *et al.* (2011) [PWY] develop a test for the presence of an explosive episode in some part of the series based on the maximum of a sequence of forward recursive augmented Dickey-Fuller [ADF] statistics. This methodology is extended by Phillips *et al.* (2015) [PSY] who develop methods, based on backward and doubly recursive sequences of ADF statistics, which have become the industry standard for detecting and date-stamping bubble episodes. Other approaches based on subsample methods include, *inter alia*, Homm and Breitung (2012), Harvey *et al.* (2015), Harvey *et al.* (2019, 2020), Astill *et al.* (2017), and Phillips and Shi (2018).

Despite many of these papers using the rational bubble model as motivation, none of them are based on the general solution of the standard stock pricing equation which decomposes the price series into the sum of two separate unobserved components: the fundamental price (the particular solution) and an unrelated bubble component. Rather, the bubble detection methods mentioned above all model the price series as a single time-varying autoregressive [TVAR] process. The null hypothesis that no bubble is present then equates to the dominant AR coefficient in this model being constant over the sample and equal to unity, while the alternative hypothesis of at least one bubble episode equates to this coefficient being greater than unity for some subset of the sample. So while extant tests have been demonstrated to exhibit strong power when prices are generated as a single TVAR process, their efficacy in detecting bubbles generated according to the general solution of the pricing equation is, as yet, largely unexplored.

A notable exception is Shi and Phillips (2023), who in their analysis of housing fever, which arises when fundamental economic factors do not justify ongoing rises in house prices, explicitly recognize this deficiency in the literature, arguing that prices "...involve fundamentals as well as the bubble process, at least when it is present, leading to a potential mismatch between the model for the data and typical empirical testing. Contamination of this type can lead to false conclusions on bubble detection" (*ibid*, p.179). They propose a method based on pre-filtering a proxy for the fundamental component out of the observed price series using an IVX regression approach of the type developed in Kostakis *et al.* (2015). Other related approaches are also discussed in section 3.2.2 of Shi and Phillips (2023). An obvious drawback of these approaches is that the set of observed variables used to proxy the fundamental component of prices may or may not be good proxies, not least because for many assets (e.g. Bitcoin) there is a lack of consensus on what constitutes the fundamental component. Their efficacy is therefore unknown in any practical application.

Other than the aforementioned methods which attempt to proxy the fundamental component, to the best of our knowledge there has been no attempt to develop tests for asset price bubbles in the context of an econometric model based on the general solution of the stock pricing equation. It is this gap in the literature that we address here. By making the standard assumption that the fundamental component follows a martingale process, and specifying the bubble component to follow an episodic explosive autoregressive process, we specify an unobserved components time series model whose components correspond to the fundamental and bubble part of the general solution of the stock pricing equation.

Within the context of this econometric model, we develop a test for the null hypothesis that a bubble component is not present in a sample of price data. As is commonly the case in the unobserved components literature, this test is based on the locally best invariant [LBI] principle. In order to obtain a statistic with a relatively simple form, this is done under the assumption of Gaussianity and with power directed against an alternative where a single bubble episode occurs within a window of known dates and with known explosive autoregressive parameter, $\rho > 1$. A feasible version of this test which does not assume known start and end dates for the explosive regime, or indeed the number of bubble regimes present, is subsequently developed. Following the same approach taken by PSY, this is based on the maximum from the sequence of such statistics formed over all possible start and end dates (subject to a minimum window width). This yields a family of test statistics indexed by ρ. In order to obtain a tractable limiting distribution theory for these statistics, we parameterize ρ to lie in the positive half of the local-to-unity region of the parameter space, such that $\rho = 1+c/O(T)$, where T is the sample size and $c > 0$ is the local explosivity parameter. Limiting distribution theory, appropriate under both the null and local (in c) alternatives, and which does not require the Gaussianity assumption to hold, is provided.

Monte Carlo methods are used to compare the finite sample properties of our proposed tests with the analogous tests from PSY. Here we also include a version of our tests which includes a modification of the variance estimate used, designed to ameliorate the impact of the termination of bubble regimes. These results highlight that our proposed tests, particularly those employing this modification, display substantially higher power to detect bubble episodes than the PSY tests for a data generating process [DGP] formed as the sum of an $I(1)$ component and a periodic bubble component. As the value of the localisation parameter, c, is unknown, the user must select a value for this, say $\bar{c}$. We investigate how power is affected by this choice and recommend a value of $\bar{c}$ to use in practice.

The paper is organized as follows. Section 2 reviews the general solution of the standard stock pricing equation and develops an unobserved components econometric model motivated by this. Section 3 develops our LBI-based tests and establishes their large sample properties. Modifications to the variance estimate used in the tests are considered in sections 4 and 6. Our Monte Carlo study is reported in section 5. Section 7 reports an empirical application for data on a range of equity indices spanning the historic dotcom episode. Here our tests are found to provide stronger evidence for the presence of bubble episodes than the PSY tests. Section 8 concludes. A supplementary appendix contains mathematical proofs, additional material relating to sections 5 and 7, and extensions allowing for a drift in the fundamental price, and for the presence of unconditional heteroskedasticity in the errors.

2 An Unobserved Components Model for Asset Prices

We first review the general solution of the standard stock pricing equation. Regardless of whether the data are measured in levels or natural logarithms, this decomposes an asset price into the sum of a fundamental component and an unrelated bubble component. Based on this decomposition we propose an unobserved components time series model for prices, applicable for either logs or levels data.

2.1 Prices

The standard no-arbitrage condition for the determination of the price, P_t, of an asset at time t, implies that it can be written as the conditional expectation of the future price,

P_{t+1}, plus dividend (or other fundamentals, such as rental value with property assets), D_{t+1}, discounted by the risk-free rate, $R > 0$; that is,

$$P_t = \frac{\mathbb{E}_t\left[P_{t+1} + D_{t+1}\right]}{1+R} \tag{1}$$

where $\mathbb{E}_t$ denotes expectation conditional on information available at time t. Beginning from $P_t = \mathbb{E}_t(P_t)$ and iterating k periods forward gives $P_t = \frac{\mathbb{E}_t[P_{t+k}]}{(1+R)^k} + \sum_{i=1}^{k} \frac{\mathbb{E}_t[D_{t+i}]}{(1+R)^i}$ and hence, as $k \to \infty$, we obtain that the general solution to (1) is given by

$$P_t = \lim_{k\to\infty} \frac{\mathbb{E}_t[P_{t+k}]}{(1+R)^k} + \sum_{i=1}^{\infty} \frac{\mathbb{E}_t[D_{t+i}]}{(1+R)^i}. \tag{2}$$

The *fundamental* price, F_t, is defined as the particular solution for P_t in (2) where the *transversality condition*, $\lim_{k\to\infty} \frac{\mathbb{E}_t[P_{t+k}]}{(1+R)^k} = 0$, holds; that is, F_t is the present value of the sum of all discounted future dividends. Notice, by definition, F_t satisfies the condition that $\lim_{k\to\infty} \frac{\mathbb{E}_t[F_{t+k}]}{(1+R)^k} = 0$. The general solution for P_t is of the form

$$P_t = F_t + B_t \tag{3}$$

where the bubble component, B_t, is unrelated to the fundamental component, F_t.

Substituting (3) into (1) and rearranging gives

$$F_t + B_t - \frac{\mathbb{E}_t[B_{t+1}]}{1+R} = \frac{\mathbb{E}_t[F_{t+1} + D_{t+1}]}{1+R}$$

from which it is seen that B_t satisfies the condition that

$$\mathbb{E}_t[B_{t+1}] = (1+R)B_t, \quad R > 0 \tag{4}$$

and is seen to be explosive in (conditional) expectation since, by the law of iterated expectations, (4) implies that $\mathbb{E}_t[B_{t+s}] = (1+R)^s B_t$. Where B_t is constrained to be non-negative (which rules out negative bubbles) the condition in (4) entails that B_t is a submartingale. Where B_t is constrained to be positive it constitutes a *rational bubble*.

2.2 Log Prices

To analyse the natural logarithms of prices, we consider the no arbitrage condition (1) for log prices; that is,

$$\log P_t = \frac{\mathbb{E}_t\left[\log(P_{t+1} + D_{t+1})\right]}{\log(1+R)}. \tag{5}$$

Campbell and Shiller (1989) develop an approximation for the numerator term $\log(P_{t+1} + D_{t+1})$, on the basis of the approximating assumption that the ratio $\phi_t := P_{t+1}/(P_{t+1} + D_{t+1})$ is constant over time, i.e. $\phi_t \simeq \phi$, with $0 < \phi < 1$. Under this approximation we obtain

$$\log(P_{t+1} + D_{t+1}) = \phi \log P_{t+1} + (1-\phi)\log D_{t+1} + h$$

where the constant h is a function of ϕ, and hence (5) can be written as:

$$\log P_t = \phi\mathbb{E}_t[\log P_{t+1}] + (1-\phi)\mathbb{E}_t[\log D_{t+1}] + c$$

where $c := h - \log(1+R)$. Iterating forwards k periods gives

$$\log P_t = c(1 + \phi + \phi^2 + ... + \phi^k) + \phi^{k+1}\mathbb{E}_t[\log P_{t+k+1}] + (1-\phi)\sum_{i=0}^{k}\phi^i\mathbb{E}_t[\log D_{t+1+i}]$$

and hence, as $k \to \infty$,

$$\log P_t = \frac{c}{1-\phi} + \lim_{k\to\infty}\phi^{k+1}\mathbb{E}_t[\log P_{t+k+1}] + (1-\phi)\sum_{i=0}^{\infty}\phi^i\mathbb{E}_t[\log D_{t+1+i}]. \tag{6}$$

In this case, log fundamentals are defined as the case where log prices depend solely on expected future dividends, which is obtained where

$$\lim_{k\to\infty}\phi^{k+1}\mathbb{E}_t[\log P_{t+k+1}] = 0 \tag{7}$$

and, hence, we find $\log P_t = \log F_t$ where

$$\log F_t := \frac{c}{1-\phi} + (1-\phi)\sum_{i=0}^{\infty}\phi^i\mathbb{E}_t[\log D_{t+1+i}]. \tag{8}$$

Again, other solutions for $\log P_t$ which lead to (8) are possible. Suppose that

$$\log P_t = \log F_t + b_t. \tag{9}$$

Substituting (9) into (6), using (7) and rearranging gives

$$\log F_t + b_t - \lim_{k\to\infty} \phi^{k+1}\mathbb{E}_t[b_{t+k+1}] = \frac{c}{1-\phi} + (1-\phi)\sum_{i=0}^{\infty}\phi^i\mathbb{E}_t[\log D_{t+1+i}].$$

Then any b_t process which satisfies $b_t - \lim_{k\to\infty}\phi^{k+1}\mathbb{E}_t[b_{t+k+1}] = 0$ implies $\log P_t = \log F_t + b_t$, with F_t satisfying (8). The necessary condition for this is that $b_t = \phi\mathbb{E}_t[b_{t+1}]$, since through forward iteration, starting from $b_t = \mathbb{E}_t(b_t)$, we find that $b_t = \lim_{i\to\infty}\phi^i\mathbb{E}_t[b_{t+i}]$; equivalently, $\mathbb{E}_t[b_{t+1}] = \frac{1}{\phi}b_t$, with $\frac{1}{\phi} > 1$. Consequently, (9) decomposes the log asset price into a log fundamental price component, $\log F_t$, and a bubble component, b_t, which, like B_t in (3), is explosive in expectation.

2.3 The Unobserved Components Time Series Model

We now turn to developing a time series model that corresponds to the general solution of the standard stock pricing equation, (2). In what follows, our analysis is based on the decomposition for prices in (3), but we note that it could equally be applied to log prices, given the equivalent decomposition implied by (9).

Based on the decomposition in (3), we specify an unobserved components model for P_t, based on an available a sample of data for $t = 1, ..., T$, of the form

$$P_t = \mu + F_t + B_t, \quad t = 1, ..., T \tag{10}$$

where μ is a constant term allowing for an arbitrary level in prices. To complete the statistical model we need to specify stochastic processes corresponding to the fundamental price, F_t, and the unrelated bubble component, B_t, in (3).

Consider F_t first. It is seen from the general solution in (2) that the behavior of F_t is determined by the character of the dividend series. A standard assumption made in the literature, dating back to Bachelier (1900), is that the fundamental price is a martingale process, such that $\mathbb{E}_{t-1}(F_t) = F_{t-1}$, with some justifications for this assumption discussed in Breitung and Kruse (2013, pp.913–914). Accordingly, we specify the component for F_t to be generated by the first-order unit root autoregression,

$$F_t = F_{t-1} + \varepsilon_t, \quad t = 1, ..., T \tag{11}$$

with $F_0 = o_p(T^{1/2})$ and where ε_t is a martingale difference [MD] process with constant variance σ^2 which is bounded and bounded away from zero.

Turning to the bubble component, B_t, in (3), as we have seen the key condition this needs to satisfy is given by (4). As discussed in Homm and Breitung (2012, pp.201-203) this allows for a wide range of possible stochastic processes, including the deterministic bubble model of Blanchard and Watson (1982), the randomly starting bubble model (outlined in Homm and Breitung, 2012, p.201), and the periodically collapsing bubble model of Evans (1991). A first-order autoregression whose lag coefficient is strictly greater than one also satisfies (4) (though it is not a submartingale), with empirical studies finding that any explosive behavior found to be present in prices tends to be episodic in nature. Because of this, we adopt a relatively simple model of episodic explosive behavior for B_t, whereby B_t is zero other than between the two unknown dates $1 \leq t_{b1} < t_{b2} \leq T$, where it follows an explosive first-order autoregression; that is,

$$B_t = \begin{cases} \rho B_{t-1} + \eta_t, & t = t_{b1}, ..., t_{b2} \\ 0 & \text{otherwise} \end{cases} \tag{12}$$

where $\rho > 1$ and η_t is a MD process, independent of ε_t, with bounded variance, ω^2.

Clearly, under the specification for B_t in (12), if $\omega^2 > 0$, there is a single explosive episode occurring between two deterministic time points, t_{b1} (the bubble inception date) and t_{b2} (the crash date). In contrast, if $\omega^2 = 0$, $B_t = 0$ for all t and the bubble component is absent from P_t. In the next section, we will develop methods, based on the LBI testing principle, for discriminating between these two cases. We will initially treat t_{b1}, t_{b2} and ρ

as known, but will subsequently relax this assumption. This will be shown to deliver tests which are based on statistics of a simple form and with tractable limiting distributions. Although, by design, the power function of these tests is directed against the specific alternative of a single explosive episode, the tests will also have power against many other more complicated alternatives, including, for example, models with multiple bubble episodes.

3 LBI-Based Tests for the Presence of a Bubble

Our aim is to develop tests for the presence of the bubble component, B_t, in the context of the unobserved components model specified for P_t in (10)–(12). This can be framed in testing

$$H_0 : \omega^2/\sigma^2 = 0 \qquad \text{vs.} \tag{13}$$

$$H_1 : \omega^2/\sigma^2 > 0. \tag{14}$$

Under H_0, $P_t = F_t$, for all t. Given the specification in (11), P_t therefore follows a random walk under the null hypothesis. Notice, therefore, that our null model coincides with the null model considered by PWY and PSY.

In section 3.1 we first use the LBI-testing principle to derive a test for H_0 against H_1 in the case where the break dates t_{b1} and t_{b2} and the autoregressive parameter, ρ, are all assumed known. Subsequently, in section 3.2, we will develop a feasible version of this test which does not require knowledge of these parameters.

3.1 An Infeasible LBI-Based Test

Consider first the infeasible case where t_{b1}, t_{b2} and ρ are all assumed known. For the purposes of deriving LBI tests of H_0 against H_1 we will additionally assume that both ε_t and η_t are Gaussian processes. The assumption of Gaussianity facilitates the construction of LBI test statistics with a simple structure; nonetheless, all of the limiting results subsequently given in section 3.3 will be shown to hold without the need for the Gaussianity assumption.

To that end, we first write the unobserved components model (10)–(12) in matrix form as $\boldsymbol{P} = \mu\mathbf{1} + \boldsymbol{F} + \boldsymbol{B}$, where $\boldsymbol{P} := (P_1, ..., P_T)'$, $\boldsymbol{F} := (F_1, ..., F_T)'$, $\boldsymbol{B} := (B_1, ..., B_T)'$, and $\mathbf{1}$ is a $(T \times 1)$ vector of 1s. Under the Gaussianty assumption, it is straightforward to show that $\boldsymbol{P} - \mu\mathbf{1} \sim N_T(\mathbf{0}, \boldsymbol{Q}(\omega^2))$ where N_k denotes a multivariate Gaussian distribution of dimension k, $\mathbf{0}$ is a $(T \times 1)$ vector of zeros, and where the variance matrix is of the form $\boldsymbol{Q}(\omega^2) := \sigma^2\boldsymbol{D} + \omega^2\boldsymbol{A}$, where $\boldsymbol{D}$ is a $(T \times T)$ matrix with (i, j)'th element $D_{i,j}$ given by $\min(i, j)$, $i, j = 1, ..., T$, and $\boldsymbol{A}$ is a $(T \times T)$ block diagonal matrix which has (i, j)'th element $A_{i,j}$ equal to 0 for $i, j \notin [t_{b1}, ..., t_{b2}]$, while for $i, j \in [t_{b1}, ..., t_{b2}]$ the sub-matrix $\boldsymbol{A}_{t_{b1}:t_{b2}}$ is given by $\boldsymbol{A}_{t_{b1}:t_{b2}} = \boldsymbol{C}_{t_{b1}:t_{b2}}\boldsymbol{C}'_{t_{b1}:t_{b2}}$ where $\boldsymbol{C}_{t_{b1}:t_{b2}}$ is a $(t_{b2} - t_{b1} + 1) \times (t_{b2} - t_{b1} + 1)$ lower triangular matrix with (i, j)'th element equal to ρ^{i-j}. For the present, ρ is taken to be a known explosive autoregressive parameter whose value is fixed and is strictly greater than one.

We can appeal directly to equation (6) of King and Hillier (1985, p.99) to obtain the critical region of the LBI test for (13) against (14) provided $\boldsymbol{Q}(0) = \sigma^2\boldsymbol{I}_T$, where $\boldsymbol{I}_k$ denotes the $k \times k$ identity matrix. However, this is clearly not the case here, and so we must first apply a transformation to the data, such that this holds. To that end, consider the data transformation $\boldsymbol{M}(\boldsymbol{P} - \mu\mathbf{1}) \sim N(0, \boldsymbol{M}\boldsymbol{Q}(\omega^2)\boldsymbol{M}')$ where $\boldsymbol{M}'\boldsymbol{M} = \boldsymbol{D}^{-1}$, so that $\boldsymbol{M}$ is a $(T \times T)$ matrix with (i, i)'th element $M_{i,i} = 1$, $i = 1, ..., T$, and $(i, i-1)$'th element $M_{i,i-1} = -1$, $i = 2, ..., T$, and all other elements equal to zero. Aside from end effects, this transformation essentially corresponds to first differencing the data; specifically, we find that $\boldsymbol{M}(\boldsymbol{P} - \mu\mathbf{1}) = [P_1 - \mu, \Delta P_2, ..., \Delta P_T]'$. It is easily seen that the covariance matrix of $\boldsymbol{M}(\boldsymbol{P} - \mu\mathbf{1})$ is given by $\boldsymbol{M}\boldsymbol{Q}(\omega^2)\boldsymbol{M}' = \sigma^2\boldsymbol{I}_T + \omega^2\boldsymbol{M}\boldsymbol{A}\boldsymbol{M}'$, and hence it follows that $\boldsymbol{M}\boldsymbol{Q}(0)\boldsymbol{M}' = \sigma^2\boldsymbol{I}_T$.

Applying the aforementioned result in King and Hillier (1985), we obtain that a LBI test of (13) against (14) rejects for large positive values of the statistic

$$S_\rho(\tau_{b1}, \tau_{b2}) := \frac{\boldsymbol{r}'\boldsymbol{M}\boldsymbol{A}\boldsymbol{M}'\boldsymbol{r}}{T^{-1}\boldsymbol{r}'\boldsymbol{r}} \tag{15}$$

where $\boldsymbol{r} := [0, \Delta P_2, ..., \Delta P_T]'$ is the vector of residuals from the OLS (null) regression of $[P_1, \Delta P_2, ..., \Delta P_T]'$ on $[1, 0, ..., 0]'$. In section A.1 of the supplementary appendix it is shown that (15) can be equivalently written in scalar notation as

$$S_\rho(\tau_{b1}, \tau_{b2}) = \frac{\sum_{t=t_{b1}+\mathbb{I}(t_{b1}=1)}^{t_{b2}} (\Delta P_t + (\rho - 1) \sum_{j=t+1}^{t_{b2}} \rho^{j-t-1} \Delta P_j)^2 + \mathbb{I}(t_{b1} = 1)((\rho - 1) \sum_{j=t_{b1}+1}^{t_{b2}} \rho^{j-t_{b1}-1} \Delta P_j)^2}{\hat{\sigma}^2}$$

where $\hat{\sigma}^2 := T^{-1} \sum_{t=2}^{T} (\Delta P_t)^2$ is a scale estimate, '$\mathbb{I}(t_{b1} = 1)$' denotes the indicator function taking the value 1 when $t_{b1} = 1$ and zero otherwise, and where $\tau_{b1} = t_{b1}/T$ and $\tau_{b2} = t_{b2}/T$.

In the first term in the numerator of $S_\rho(\tau_{b1}, \tau_{b2})$, ΔP_t can be shown to be of a lower stochastic order of magnitude than $(\rho - 1) \sum_{j=t+1}^{t_{b2}} \rho^{j-t-1} \Delta P_j$. We therefore choose in what follows to work with a simplified version of the $S_\rho(\tau_{b1}, \tau_{b2})$ statistic that omits this lower order term. After re-arranging the remaining terms, this yields the statistic, $S_\rho^*(\tau_{b1}, \tau_{b2})$, given by:

$$S_\rho^*(\tau_{b1}, \tau_{b2}) := \frac{(\rho - 1)^2 \sum_{t=t_{b1}+1}^{t_{b2}} \left(\sum_{j=t}^{t_{b2}} \rho^{j-t} \Delta P_j \right)^2}{\hat{\sigma}^2}. \tag{16}$$

Unreported simulation evidence suggests that there is essentially no loss in finite sample power from basing our proposed feasible tests, developed next in section 3.2, on this simplified version of the LBI statistic.

Remark 3.1. Both the LBI test of (13) against (14) based on the $S_\rho(\tau_{b1}, \tau_{b2})$ statistic in (15), and the analogous test based on the simplified statistic $S_\rho^*(\tau_{b1}, \tau_{b2})$ in (16), are invariant under the group of transformations $\boldsymbol{P} \to \gamma_0 \boldsymbol{P} + \gamma_1$, $\mu \to \gamma_0 \mu + \gamma_1$ and $\sigma^2 \to \gamma_0^2 \sigma^2$, where γ_0 is a non-zero scalar and γ_1 is a scalar. ◇

3.2 Feasible Implementation of the Test

In practice the value of the explosive autoregressive parameter, ρ, and the timing of the bubble start and end dates, t_{b1} and t_{b2}, will be unknown to the practitioner. Consequently, in this section we develop a feasible version of the test based on the statistic in (16), which does not require knowledge of these parameters.

To that end, corresponding to arbitrary possible start and end dates, denoted $t_1 = \lfloor \tau_1 T \rfloor$ and $t_2 = \lfloor \tau_2 T \rfloor$, respectively (which may or may not coincide with the true dates t_{b1} and t_{b2}), we can define the generic sub-sample statistic, $S_\rho^*(\tau_1, \tau_2)$, to be of the form given in (16) but computed over the sub-sample $t = t_1, ..., t_2$. Since the true bubble start and end dates are unknown, and following the same approach as that taken by PSY in the context of sub-sample ADF statistics, we can then base a test on the statistic that takes the maximum value of $S_\rho^*(\tau_1, \tau_2)$ across all possible bubble timings, subject to a constraint on the minimum permitted bubble regime length.

This supremum statistic is, however, still infeasible in the absence of knowledge of ρ. A feasible version can though be obtained by specifying a value of this parameter to use, which again may or may not be equal to the true value of ρ. We denote this value by $\bar{\rho} > 1$. In order to obtain a supremum statistic for which a tractable asymptotic distribution can be derived, we set $\bar{\rho}$ to be local-to-unity, with the scaling appropriate to the sub-sample size that the numerator of the statistic is based upon. Specifically we set

$$\bar{\rho} = \bar{\rho}_T = 1 + \bar{c}(t_2 - t_1)^{-1}, \quad \bar{c} > 0 \tag{17}$$

where $\bar{c}$ is a user-specified positive constant.

Our feasible test then rejects for large (positive) values of the supremum statistic

$$S_{\bar{c}}^* \quad := \sup_{\tau_1 \in [1/T, 1-\pi]} \sup_{\tau_2 \in [\tau_1 + \pi, 1]} \log S_{\bar{c}}^*(\tau_1, \tau_2) \tag{18}$$

where

$$S_{\bar{c}}^*(\tau_1, \tau_2) := \frac{\bar{c}^2 (t_2 - t_1)^{-2} \sum_{t=t_1+1}^{t_2} \left(\sum_{j=t}^{t_2} \{1 + \bar{c}(t_2 - t_1)^{-1}\}^{j-t} \Delta P_j \right)^2}{\hat{\sigma}^2} \tag{19}$$

and where $\lfloor \pi T \rfloor$ represents some minimum permitted value for the sub-sample length, $t_2 - t_1$. Notice that, as a practical convenience, because of the exponential nature of the sub-sample statistics involved we have applied a log transformation to $S^*_{\bar{c}}(\tau_1, \tau_2)$ in the supremum statistic in (18). Being a monotonic transformation, this has no impact on the critical region of the test.

Remark 3.2. The test based on $S^*_{\bar{c}}$ is the analogue in our setting of the $GSADF$ test outlined on pp.1048–49 of PSY. These authors also discuss tests designed for detecting a single bubble episode based on the suprema of sequences of forward and backward recursive subsample ADF statistics, labelled $SADF$ (which coincides with the test proposed in PWY) and $BSADF$; see PSY p.1048 and pp.1051–52, respectively. Although we will not consider such tests here, analogues of the $SADF$ and $BSADF$ tests in our setting can be defined as those tests which reject for large values of the statistics $FS^*_{\bar{c}} := \sup_{\tau_2 \in [1/T+\pi, 1]} \log S^*_{\bar{c}}(\frac{1}{T}, \tau_2)$ and $BS^*_{\bar{c}}(\tau_2) := \sup_{\tau_1 \in [1/T, \tau_2 - \pi]} \log S^*_{\bar{c}}(\tau_1, \tau_2)$, for some $\tau_2 \in (\pi, 1]$, respectively. $\diamondsuit$

3.3 Limiting Distribution Theory

We next derive the large sample behavior of $S^*_{\bar{c}}$ of (18) under both H_0 and H_1. As with $\bar{\rho}$, discussed above, we will treat ρ as local-to-unity in order that a tractable asymptotic distribution for $S^*_{\bar{c}}$ can be obtained. Specifically, and analogously to (17), we set

$$\rho = \rho_T = 1 + c(t_{b2} - t_{b1})^{-1}, \quad c > 0. \tag{20}$$

Regularity conditions are also needed for the innovations, ε_t and η_t. These are now stated in Assumption 1.

Assumption 1. *We assume that ε_t and η_t are independent MD sequences, each with finite fourth moments. Furthermore, $E(\varepsilon_t^2) = \sigma^2$, where σ^2 is bounded and bounded away from zero, and $E(\eta_t^2) = \omega^2$, where ω^2 is bounded.*

Remark 3.3. Notice that Assumption 1 does not impose Gaussianity on either ε_t or η_t. Moreover, Assumption 1 allows for a wide class of models of conditional heteroskedasticty in both η_t and ε_t, including ARCH and GARCH models. Assumption 1 does, however, impose unconditional homosekdasticity on both η_t and ε_t. While unconditional heteroskedasticity in only η_t would not affect the limiting null distribution of the $S^*_{\bar{c}}$ statistic, it would have an impact on the local power of the test. Generalisations to allow for unconditional heteroskedasticity in ε_t and/or η_t, including wild bootstrap implementations of the tests proposed in section 3.2, are detailed in section A.2 of the supplementary appendix. $\diamond$

The limiting distribution of $S^*_{\bar{c}}$ of (18) under the alternative hypothesis H_1 of (14) when ρ and $\bar{\rho}$ are local, satisfying (20) and (17), respectively, is now provided in Theorem 1. Corollary 1 subsequently gives the limiting null distribution of $S^*_{\bar{c}}$.

Theorem 1. *Let the data be generated by (10)–(12) and let Assumption 1 hold. Then under H_1 of (14), with ρ and $\bar{\rho}$ satisfying (20) and (17), respectively, we have that, as $T \to \infty$,*

$$S^*_{\bar{c}} \xrightarrow{w} \sup_{\tau_1 \in [0,1-\pi]} \sup_{\tau_2 \in [\tau_1+\pi,1]} \log H_{c,\bar{c}}(\tau_1, \tau_2, \omega/\sigma, \tau_{b1}, \tau_{b2})$$

where '$\xrightarrow{w}$' denotes weak convergence, and where

$$H_{c,\bar{c}}(\tau_1, \tau_2, \omega/\sigma, \tau_{b1}, \tau_{b2}) := \frac{N_{c,\bar{c}}(\tau_1, \tau_2, \omega/\sigma, \tau_{b1}, \tau_{b2})}{1 + \left(\frac{\omega}{\sigma}\right)^2 (\tau_{b2} - \tau_{b1}) + \left(\frac{\omega}{\sigma}\right)^2 \left\{\int_{\tau_{b1}}^{\tau_{b2}} e^{c(\tau_{b2}-s)(\tau_{b2}-\tau_{b1})^{-1}} dW_\eta(s)\right\}^2}$$

with

$$N_{c,\bar{c}}(\tau_1, \tau_2, \omega/\sigma, \tau_{b1}, \tau_{b2}) := \bar{c}^2(\tau_2-\tau_1)^{-2} \int_{\tau_1}^{\tau_2} \left\{\int_r^{\tau_2} e^{\bar{c}(s-r)(\tau_2-\tau_1)^{-1}} dK_c(s, \omega/\sigma, \tau_{b1}, \tau_{b2})\right\}^2 dr$$

and

$$K_c(r, \omega/\sigma, \tau_{b1}, \tau_{b2}) := W_\varepsilon(r) + \mathbb{I}(\tau_{b1} \leq r \leq \tau_{b2}) \frac{\omega}{\sigma} \int_{\tau_{b1}}^{r} e^{c(r-s)(\tau_{b2}-\tau_{b1})^{-1}} dW_\eta(s) \qquad (21)$$

where $W_\varepsilon(r)$ and $W_\eta(r)$ are independent standard Brownian motions.

Corollary 1. *The limiting distribution of* $S^*_{\bar{c}}$ *under* H_0 *of* (13) *follows directly from the result in Theorem* 1*, on setting* $\omega^2 = 0$*. That is,*

$$S^*_{\bar{c}} \xrightarrow{w} \sup_{\tau_1 \in [0, 1-\pi]} \sup_{\tau_2 \in [\tau_1 + \pi, 1]} \log L_{\bar{c}}(\tau_1, \tau_2)$$

where

$$L_{\bar{c}}(\tau_1, \tau_2) := \bar{c}^2 (\tau_2 - \tau_1)^{-2} \int_{\tau_1}^{\tau_2} \left\{ \int_r^{\tau_2} e^{\bar{c}(s-r)(\tau_2 - \tau_1)^{-1}} dW_\varepsilon(s) \right\}^2 dr.$$

Remark 3.4. The result in Theorem 1 establishes that the test based on $S^*_{\bar{c}}$ has non-trivial asymptotic local power under H_1 in the case where a single bubble episode occurs in the data, as in (12). The local limiting power function of the test in this case is seen to depend on the (unknown) start and end dates of the bubble window, τ_{b1} and τ_{b2} respectively, the innovation variance ratio, ω^2/σ^2, and on both the unknown true explosive parameter, ρ (through c), and the user-selected value $\bar{\rho}$ (through $\bar{c}$). We will explore the impact of these parameters on test power in our numerical simulations in section 5. The result in Corollary 1 shows that, of the nuisance parameters affecting the local limiting power function, only $\bar{c}$ also features in the limiting null distribution of $S^*_{\bar{c}}$. ♢

Remark 3.5. The local power result given in Theorem 1 relates to the single bubble model in (12). In the case where further bubble episodes are present, additional terms relating to these further episodes will appear in both the denominator of $H_{c,\bar{c}}(\tau_1, \tau_2, \omega/\sigma, \tau_{b1}, \tau_{b2})$ and on the right member of (21). The latter will be analogous to the second term on the right member of (21), but defined to be non-zero over the subsamples of the data containing the additional bubbles. As such, the test based on $S^*_{\bar{c}}$ will also have non-trivial asymptotic local power against models featuring multiple bubble episodes. Power in a case where two bubble episodes are present will also be explored in our simulations in section 5. ♢

Remark 3.6. Thus far we have assumed that the fundamental price, F_t, is generated as a driftless random walk process. It is possible, however, that F_t could follow a random walk with drift, as for example happens if dividends, D_t, follow a random walk with drift; see Breitung and Kruse (2013, p.913-914). In this case a drift term, μ_F, is added to the right hand side of (11). Here $S^*_{\bar{c}}$ of (18) is not invariant to linear translations of the form $\boldsymbol{P} \rightarrow \gamma_0 \boldsymbol{P} + \gamma_1 + \gamma_2 t$, where γ_0 is a non-zero constant and γ_j, $j = 1, 2$, are constants; in particular, it will depend on the value of the drift term, μ_F. To obtain a statistic which is invariant to such linear translations (and, hence, does not depend on μ_F), we simply replace ΔP_t in both the numerator of (19) and in the variance estimate, $\hat{\sigma}^2$, by its de-meaned equivalent, $\Delta P_t - (T-1)^{-1} \sum_{t=2}^{T} \Delta P_t$. This will alter the limiting distribution of $S^*_{\bar{c}}$ *vis-à-vis* Theorem 1 and Corollary 1. Specifically, the standard Brownian motion $W_\varepsilon(r)$ needs to be replaced by the Brownian bridge, $W_\varepsilon(r) - rW_\varepsilon(1)$, and if under the alternative H_1 the bubble runs to the end of the sample, an additional term appears in the definition of $K_c(r, \omega/\sigma, \tau_{b1}, \tau_{b2})$ of (21). Further details regarding the de-meaned variant of the test are presented in section A.4 of the supplementary appendix. $\diamondsuit$

4 A Modification to the Variance Estimate

As is implicit in the proof of Theorem 1, under H_0, $\hat{\sigma}^2$ in (19) is a consistent estimate of σ^2, the variance of the innovation driving the fundamental price, ε_t. We now detail a simple modification to $\hat{\sigma}^2$, related to removing the impact of the one-period outlier that appears in the first differences of prices under H_1 immediately after a bubble regime terminates.

It is clear from the DGP in (10)–(12) that when a bubble episode terminates, a level shift occurs as the series returns from $P_t = \mu + B_t + F_t$ to $P_t = \mu + F_t$. This induces a one-time outlier in the first differences of P_t , such that $\Delta P_{t_{b2}+1}$ is of $O_p(T^{1/2})$ (see the proof of Theorem 1). Indeed, this term is responsible for the third term in the denominator of

$H_{c,\bar{c}}(\tau_1, \tau_2, \omega/\sigma, \tau_{b1}, \tau_{b2})$. It is therefore to be expected that the power of the test based on $S^*_{\bar{c}}$ would be increased by removing this outlier from the calculation of the scale estimator, $\hat{\sigma}^2$, in the denominator of $S^*_{\bar{c}}(\tau_1, \tau_2)$.

To that end, we note that, for large T, $\max_{t\in[2,\ldots,T]} |\Delta P_t| = |\Delta P_{t_{b2}+1}|$ almost surely, since all of the other $|\Delta P_t|$ are of $O_p(1)$. We therefore consider a version of the $S^*_{\bar{c}}(\tau_1, \tau_2)$ statistic where we remove the largest absolute value of ΔP_t from the calculation of $\hat{\sigma}^2$; that is, we replace $\hat{\sigma}^2$ in the denominator of (19) with the modified version

$$\hat{\sigma}^2_m := T^{-1} \left\{ \sum_{t=2}^{T} (\Delta P_t)^2 - \max_{t\in[2,\ldots,T]} |\Delta P_t|^2 \right\}. \tag{22}$$

It is straightforward to show that under H_1 of (14) that $\hat{\sigma}^2_m \xrightarrow{p} \sigma^2 + \omega^2(\tau_{b2} - \tau_{b1})$, and, hence, remains a consistent estimate of σ^2 under H_0 of (13). Under this modification, we reject H_1 for large values of the statistic

$$S^\dagger_{\bar{c}} := \sup_{\tau_1\in[1/T,1-\pi]} \sup_{\tau_2\in[\tau_1+\pi,1]} \log S^\dagger_{\bar{c}}(\tau_1, \tau_2) \tag{23}$$

where

$$S^\dagger_{\bar{c}}(\tau_1, \tau_2) := \frac{\bar{c}^2 (t_2 - t_1)^{-2} \sum_{t=t_1+1}^{t_2} \left(\sum_{j=t}^{t_2} \{1 + \bar{c}(t_2 - t_1)^{-1}\}^{j-t} \Delta P_j \right)^2}{\hat{\sigma}^2_m} \tag{24}$$

The limiting distribution of $S^\dagger_{\bar{c}}$ of (23) follows straightforwardly from the results in Theorem 1 and is now given in Corollary 2.

Corollary 2. *Let the conditions of Theorem 1 hold. Then under H_1 of (14), with ρ and $\bar{\rho}$ satisfying (20) and (17), respectively, we have that, as $T \to \infty$,*

$$S^\dagger_{\bar{c}} \xrightarrow{w} \sup_{\tau_1\in[0,1-\pi]} \sup_{\tau_2\in[\tau_1+\pi,1]} \log G_{c,\bar{c}}(\tau_1, \tau_2, \omega/\sigma, \tau_{b1}, \tau_{b2})$$

where

$$G_{c,\bar{c}}(\tau_1, \tau_2, \omega/\sigma, \tau_{b1}, \tau_{b2}) := \frac{N_{c,\bar{c}}(\tau_1, \tau_2, \omega/\sigma, \tau_{b1}, \tau_{b2})}{1 + \left(\frac{\omega}{\sigma}\right)^2 (\tau_{b2} - \tau_{b1})}. \tag{25}$$

Remark 4.1. It is seen from the results of Corollaries 1 and 2 that the limiting null distributions of the $S_{\bar{c}}^{\dagger}$ and $S_{\bar{c}}^{*}$ statistics coincide. $\diamondsuit$

Remark 4.2. If it were suspected that up to some finite number, $k \geq 1$, of terminating bubble episodes were present in the series, then it would be appropriate to account for the k possible outliers present in ΔP_t, corresponding to each of these bubble end dates. In this case the modification outlined above could be easily generalized to remove the k largest absolute values of ΔP_t from the calculation of $\hat{\sigma}^2$. Again, the resulting statistic will have the same limiting null distribution as $S_{\bar{c}}^{*}$. $\diamondsuit$

5 Finite Sample Simulations

We next report the results of a Monte Carlo simulation exercise examining the finite sample properties of our proposed $S_{\bar{c}}^{*}$ and $S_{\bar{c}}^{\dagger}$ tests, together with the $GSADF$ test of PSY, each compared to 5% level finite sample critical values generated via simulation with $\omega = 0$. The regressions underlying the $GSADF$ statistic are implemented with an intercept and no corrections for weak dependence are made to any of the $S_{\bar{c}}^{*}$, $S_{\bar{c}}^{\dagger}$ or $GSADF$ statistics. We apply a minimum window width setting of $\pi = 0.1$ for the $S_{\bar{c}}^{*}$, $S_{\bar{c}}^{\dagger}$ and $GSADF$ statistics.

We first examine the case of a single bubble episode with data generated according to (10)–(12) with $T = 200$, $\varepsilon_t \sim NIID(0,1)$, $\eta_t \sim NIID(0,\omega^2)$ and $\rho = 1+c(t_{b2}-t_{b1})^{-1}$, with the start and end dates of the bubble episode given by t_{b1} and t_{b2}, respectively. We report the rejection frequencies of the tests across a grid of values of ω, with $\omega = 0$ corresponding to the null of no bubble and $\omega > 0$ generating a bubble episode in the price series, P_t, under the alternative. In order that the simulated bubble episodes represent upwards (positive) rather than downwards (negative) bubbles, we multiply the generated B_t component by -1 whenever $B_{t_{b2}} - B_{t_{b1}} < 0$. Corresponding to the autoregressive parameter in the bubble component in (12), we consider the range of values $c \in \{0.5, 1, 2, 4\}$, and for the choice parameter, $\bar{c}$, used to construct the $S^*_{\bar{c}}$ and $S^\dagger_{\bar{c}}$ statistics, we consider the range of values $\bar{c} \in \{2, 4, 6, 8, 10\}$. The simulations reported in this section are all based on 5000 Monte Carlo replications. In the context of the $S^\dagger_{\bar{c}}$ tests of section 4, the largest absolute value of ΔP_t was removed in calculating the modified variance estimate, $\hat{\sigma}^2_m$ of (22).

Figure 1 reports results relating to a mid-sample bubble episode where $\tau_1 = 0.3$, $\tau_2 = 0.7$ and $c \in \{1, 2, 4\}$. For $c = 1$ we see from panel (a) that the $S^*_{\bar{c}}$ tests deliver substantially higher power than the $GSADF$ test, irrespective of the choice of $\bar{c}$; for example, for $\omega = 2$ the $GSADF$ test has power of just over 20%, while the powers of the $S^*_{\bar{c}}$ tests range between around 50% for S^*_{10} and 65% for S^*_4. Among the $S^*_{\bar{c}}$ tests, the best power is offered by the S^*_4 test. In panel (b) we see that the $S^\dagger_{\bar{c}}$ tests are each somewhat more powerful than their $S^*_{\bar{c}}$ counterparts (in the foregoing example, the powers of the $S^\dagger_{\bar{c}}$ tests range between around 65% for $S^\dagger_{10}$ and 75% for $S^\dagger_4$), as would be expected from the discussion in section 4, with the best power levels again obtained by using the $S^\dagger_4$ test. The power differentials between the $S^\dagger_{\bar{c}}$ tests are, however, seen to be much smaller than those between the $S^*_{\bar{c}}$ tests in panel (a). Qualitatively similar results are seen for $c = 2$ in panels (c) and (d) and $c = 4$ in panels (e) and (f) although the power differentials between all of the tests, while preserved, are seen to diminish as the value of c increases. In summary, the $S^\dagger_4$ test is the best performing test for the DGP settings reported in Figure 1, while the $GSADF$ test performs least well.

Corresponding results for a bubble episode occurring early in the sample, with $\tau_1 = 0.2$ and $\tau_2 = 0.4$ and $c \in \{0.5, 1, 2\}$, are reported in Figure 2. Here, the values of c are half those reported for Figure 1; given the bubble length is half that used in the Figure 1 results, this ensures the same settings for the bubble magnitude $\rho = 1 + c(t_{b2} - t_{b1})^{-1}$ are employed in both cases. These results follow broadly similar patterns to those observed from Figure 1, with the $S^\dagger_{\bar{c}}$ tests again outperforming the $S^*_{\bar{c}}$ tests, and the $GSADF$ test again displaying the worst overall power profile (albeit with the $GSADF$ test displaying greater power than the S^*_{10} test for larger values of ω). Across the scenarios considered, the best power is again displayed by the $S^\dagger_4$ test.

Figure 3 reports results for a late bubble episode, with $\tau_1 = 0.8$, $\tau_2 = 1$ and $c \in \{0.5, 1, 2\}$. As the bubble episode runs to the end of the sample, there is no crash in this DGP. We observe that there is now very little difference in performance between the $S^*_{\bar{c}}$ and $S^\dagger_{\bar{c}}$ tests, highlighting that there is no apparent loss in power, relative to $S^*_{\bar{c}}$, from using the $S^\dagger_{\bar{c}}$ test in the case where no crash is present. Moreover, whatever the value of c, the powers of these tests are now also very similar across $\bar{c}$, so the particular choice of $\bar{c}$ is less important here than in the previous cases. It is, however, important to note that all of our proposed $S^\dagger_{\bar{c}}$ and $S^*_{\bar{c}}$ tests are again significantly more powerful than the $GSADF$ test.

We next examine the case where two distinct bubble episodes are present in the price series. In this case we generate the bubble component, B_t, according to:

$$B_t = \begin{cases} \rho B_{t-1} + \eta_t & t = t_{b11}, ..., t_{b21} \text{ and } t = t_{b12}, ..., t_{b22} \\ 0 & \text{otherwise} \end{cases} \tag{26}$$

where $t_{bij} = \lfloor \tau_{i,j} T \rfloor$ $i, j = 1, 2$ with $0 < \tau_{1,1} < \tau_{2,1} < \tau_{1,2} < \tau_{2,2} < 1$. We again ensure each simulated bubble episode is an upwards bubble by multiplying the relevant sub-sample component of B_t by -1 whenever $B_{t_{b21}} - B_{t_{b11}} < 0$ or $B_{t_{b22}} - B_{t_{b12}} < 0$. We consider the case where the first bubble episode manifests in the first half of the sample with a second bubble episode subsequently occurring in the second half of the sample, by setting $\tau_{1,1} = 0.2$, $\tau_{2,1} = 0.4$, $\tau_{1,2} = 0.6$ and $\tau_{2,2} = 0.8$. The bubble episodes are driven by a common explosive AR parameter $\rho = 1 + c(t_{b21} - t_{b11})^{-1}$. In the context of the $S^\dagger_{\bar{c}}$ tests, the two largest absolute values of ΔP_t were removed in calculating the modified variance estimate, $\hat{\sigma}^2_m$. Results for this scenario for $c \in \{0.5, 1, 2\}$ are reported in Figure 4. Among the $S^*_{\bar{c}}$ tests the best overall power is again displayed by the S^*_4 test, but in contrast to the previous single bubble episode scenarios the relative power of the $GSADF$ test is much stronger, particularly for the lower values of c, with the power curve of the $GSADF$ test eventually crossing those of the $S^*_{\bar{c}}$ tests for larger values of ω. The $S^\dagger_{\bar{c}}$ tests, on the other hand, continue to significantly outperform the $GSADF$ test, with the best power profile again offered by the $S^\dagger_4$ test.

Given that the best power performance was consistently found to be obtained for the $S^\dagger_4$ test, we recommend this test for practical applications. In Table 1 we report finite sample and asymptotic critical values for $S^\dagger_4$, along with S^*_4, using $\pi = 0.1$, with finite sample values reported for cases where the k largest absolute values of ΔP_t are removed when calculating $\hat{\sigma}^2_m$, with $k = \{1, 2, 3\}$. The asymptotic critical values are obtained by simulating the limiting functionals in Corollary 1 using $NIID(0, 1)$ random variates and a discretisation of 1000 steps.

Finally, we consider the case where the price series, instead of being generated by the unobserved components based DGP, (10)–(12), instead follows a univariate time-varying first-order autoregressive process of the form considered by PSY. This can be considered as a check as to whether anything is lost by performing our proposed tests when the true DGP is of the form that has most often been considered in the econometric bubble testing literature. We consider three DGPs, the first where the price series, P_t, begins as a unit root process before an explosive autoregressive phase occurs and subsequently the price series reverts to a unit root process until the end of the sample; a second where the bubble ends in a stationary collapse before unit root behavior resumes; a third where the collapse is an instantaneous crash, before reverting to a unit root process. Details of these simulation DGPs and the results for our recommended S^*_4 and $S^\dagger_4$ tests and for the $GSADF$ test, are given in section A.5 of the supplementary appendix. In the first two scenarios we find essentially no difference between the powers of the S^*_4 and $S^\dagger_4$ tests which are both marginally more powerful than $GSADF$. For the third scenario of an instantaneous crash, S^*_4 and $S^\dagger_4$ again display very similar power functions with both now significantly more powerful than

$GSADF$. These findings are reassuring, pointing to the flexibility of our proposed tests to detect bubbles generated by mechanisms outside of their natural environment.

6 Allowing for Weakly Dependent Errors

Thus far we have assumed that the fundamental price component follows a random walk (possibly with drift), implying that under H_0 of (13) the changes in prices, ΔP_t, are serially uncorrelated. While this assumption is standard in the literature, in practice there might be a degree of weak autocorrelation present in ΔP_t under the null. This could arise, for example, from the presence of weak dependence in the shocks, ε_t, driving the fundamental component in (11), or from observed transaction prices being subject to an additive weakly autocorrelated $[I(0)]$ measurement error (microstructure noise) arising from imperfections in the trading process; for the latter see, *inter alia*, Aït-Sahalia and Yu (2009).

In both of the examples above, applying first differences to (10) we obtain that

$$\Delta P_t = \Delta B_t + u_t,\ t = 2, ..., T \tag{27}$$

where u_t is an $I(0)$ series. To allow for weak dependence in u_t we assume that u_t satisfies the mixing conditions given in, for example, Assumption $\mathcal{E}$ of Cavaliere and Taylor (2005,p.1114). As discussed in Cavaliere and Taylor (2005,p.1115), this allows u_t to belong to a wide class of weakly dependent (and conditionally heteroskedastic) stationary processes, including most stationary and invertible $ARMA$ processes.

Denoting the long-run variance of u_t as $\lambda^2 := \sum_{k=-\infty}^{\infty} \mathbb{E}(u_t u_{t+k})$, it is easy to show that the limiting null distribution of $S_{\bar{c}}^*$ of (18) depends on both λ^2 and the short-run variance of u_t when u_t is weakly dependent. This arises because the estimator $\hat{\sigma}^2$ in (19) is a consistent estimate of the short-run variance of u_t, which only coincides with the long-run variance if u_t is serially uncorrelated. In order to recover the limiting null distribution of $S_{\bar{c}}^*$ given in Corollary 1 in cases where u_t is weakly dependent, we can use the same solution as outlined in the context of the LBI test of Nyblom and Mäkeläinen (1983) by Kwiatkowski *et al.* (1992) [KPSS]. This entails replacing the short run variance estimator, $\hat{\sigma}^2$, in (19) with a consistent estimate of the long run variance, λ^2, under the null.

To that end, following KPSS, we will use the familiar kernel-based estimate

$$\hat{\lambda}^2 := \sum_{j=-T+1}^{T-1} k\left(\frac{j}{q_T}\right)\hat{\gamma}(j), \quad \hat{\gamma}(j) := T^{-1}\sum_{t=|j|+2}^{T} \Delta P_t \Delta P_{t-|j|} \tag{28}$$

where q_T and $k(\cdot)$ are the bandwidth and kernel function, respectively, assumed to satisfy standard regularity conditions, such as Assumption $\mathcal{K}$ of Cavaliere and Taylor (2005,p.1115). As demonstrated in Cavaliere and Taylor (2005), these conditions ensure that $\hat{\lambda}^2 \xrightarrow{p} \lambda^2$ under H_0 (where $\Delta P_t = u_t$). Consequently, a modified statistic, which replaces $\hat{\sigma}^2$ with $\hat{\lambda}^2$ in (19) will have the same limiting null distribution as that given for $S_{\bar{c}}^*$ in Corollary 1. Correcting for weak dependence in the errors in the context of the previous modification to allow for outliers arising from bubble terminations (section 4) follows in an obvious fashion, and we denote the long-run variance estimate in this case as $\hat{\lambda}_m^2$.

We conclude this section with a short Monte Carlo study into how well these modifications of our preferred S_4^* and $S_4^\dagger$ tests (again setting $\pi = 0.1$ and removing the single largest absolute value of ΔP_t in calculating the variance estimates used in $S_4^\dagger$) perform in practice. To that end, we simulated data from (10)–(12) under H_0 of (13) with $\varepsilon_t = \varphi\varepsilon_{t-1} + e_t$ where $e_t \sim NIID(0,1)$. Table 2 reports the empirical size, again based on $5,000$ Monte Carlo replications, of $S_4^\dagger$ and S_4^* and the modifications of these based on the long-run variance estimates, $\hat{\lambda}^2$ and $\hat{\lambda}_m^2$, respectively, for $T \in \{100, 200, 400\}$ and $\varphi \in \{0, 0.3, 0.5, 0.7, 0.9\}$. In the context of $\hat{\lambda}^2$ and $\hat{\lambda}_m^2$, we use the quadratic spectral kernel with the automatic bandwidth selection method of Andrews (1991). In (28) we used de-meaned values of ΔP_t in calculating the autocovariance estimates, as this led to improved performance. The tests are compared against the 5% critical values from Table 1.

The results in Table 2 show that, as would be expected, the original S_4^* and $S_4^\dagger$ tests display severe size distortions where $\varphi \neq 0$. However, the modifications of these tests to allow for weak dependence perform remarkably well in restoring empirical size close to the nominal level. The only exception of note is for $\varphi = 0.9$ when $T = 100$ where the tests are still somewhat oversized. However, $\varphi = 0.9$ implies the changes in prices are close to being $I(1)$, arguably well beyond the level of dependence that might be anticipated in practice.

7 Empirical Illustration

In this section we report an empirical illustration of the tests outlined in the paper to a number of well known stock indices for data spanning the so called dotcom bubble. Specifically, we will test for the presence of asset price bubbles in the FTSE100, DAX, CAC 40, Nikkei, NYSE Composite, S&P500, Dow Jones Industrial Average, NASDAQ 100, NASDAQ Composite, NASDAQ Computer, NASDAQ Biotech and NASDAQ Telecoms indices using weekly data from 01/01/1995-30/12/2001 ($T = 366$). The FTSE100 data were obtained from `www.marketwatch.com`, while the remaining data were obtained from `www.investing.com`. All of the series are graphed in section A.6 of the supplementary appendix.

We begin by investigating if the constant unconditional variance assumption appears reasonable. To that end, we apply the $\mathcal{H}_{AD}$ stationary volatility test of Cavaliere and Taylor (2008, pp.311-312) which tests the null hypothesis of unconditional homoskedasticity against the alternative of non-stationary volatility. This test was applied to the first differences of the logs of each of the indices, using a Bartlett long run variance estimator with lag truncation parameter 4. The test results are reported in Table 3. The results are striking, with the test rejecting the null of constant unconditional volatility at at least the 10% level for all of the indices, excepting the Nikkei. For the five Nasdaq series the test rejects at the 1% level. Although this test will likely over-reject the null if bubble episodes are present, the consistent and in many cases highly significant rejections at the very least caution against assuming that these indices display constant unconditional variance.

Next in Table 3 we report the outcomes of asset price bubble tests in these log indices. Bootstrap p-values are reported for both our preferred $S_4^\dagger$ test and the $GSADF$ test of PSY. Both wild bootstrap p-values (designed to be robust to any unconditional heteroskedasticity present in the series) and parametric bootstrap p-values (which are not robust to unconditional heteroskedasticity) are reported. For $S_4^\dagger$, the former are obtained using Algorithm A.1, together with the adjustment discussed in Remark A.2.4, in section A.2 of the supplementary appendix, while for the $GSADF$ test they are obtained using the wild bootstrap algorithm detailed in Harvey *et al.* (2020,pp.137–138). For both $S_4^\dagger$ and $GSADF$ the parametric bootstrap p-values are obtained by Monte Carlo simulation assuming $NIID(0,1)$ shocks. All bootstraps are based on $B = 1000$ bootstrap replications. In the context of the $S_4^\dagger$ test, we remove the single largest absolute value of ΔP_t in calculating the variance estimate, and the correction for weak dependence outlined in section 6 was employed using the same kernel and bandwidth rule as used in the simulations reported in section 6. For all of the tests we set $\pi = 0.1$ so that the minimum window width is equal to 36. The $GSADF$ statistic was implemented with an intercept and one lagged dependent variable included.

Consider first the results in Table 3 relating to the heteroskedasticity-robust wild bootstrap $S_4^\dagger$ and $GSADF$ tests. For the Nikkei, NASDAQ Composite and NASDAQ Computer indices the p-values for both tests are in excess of 0.1 indicating that neither test finds evidence for an asset price bubble in these series at a standard level of significance. For the NASDAQ Biotechnology index, evidence of an explosive episode is found at the 5% level using either the $S_4^\dagger$ test or $GSADF$ test. For the remaining 8 indices, the $GSADF$ test does not detect any explosive episodes at even the 10% level, whereas $S_4^\dagger$ finds (often strongly) statistically significant evidence of explosivity for all of these series. These results are consistent with the findings of the Monte Carlo simulation study in Section 5 which found that the $S_4^\dagger$ can display often substantially higher power than the $GSADF$ test.

The parametric bootstrap p-values in Table 3 provide significantly more evidence against the null hypothesis than the corresponding wild bootstrap p-values across these indices in all but the case of the $S_4^\dagger$ test for the Nikkei index. As with the wild bootstrap tests, the results for $S_4^\dagger$ again provide a stronger body of evidence against the null than the $GSADF$ test. However, and as discussed above, the parametric bootstrap p-values should be treated with some caution in light of the results for the stationary volatility tests in Table 3.

8 Conclusions

We have proposed new methods, based on the locally best invariant testing principle, for detecting asset price bubbles in an unobserved components model whose components correspond to the fundamental price and bubble components of the general solution of the standard stock pricing equation. This model formulation contrasts with previous bubble detection tests in the literature which assume that the asset price follows a univariate time-varying autoregressive [TVAR] model. Simulation results highlighted the, often very significantly, higher power of these tests, relative to the industry standard $GSADF$ test of Phillips *et al.* (2015), for price series generated by this unobserved components model. Our proposed tests were also shown to have similar or better power than the $GSADF$ test in the case where the price series evolved according to a univariate TVAR. For data spanning the well-known dotcom bubble episode, an empirical example to a number of equity indices demonstrated that our proposed tests delivered stronger and more consistent evidence of the presence of an explosive episode than does the $GSADF$ test.

References

Aït-Sahalia, Y. and Yu, J. (2009) High frequency market microstructure noise estimates and liquidity measures. The Annals of Applied Statistics 3, 422–457.

Andrews, D.W.K. (1991). Heteroskedasticity and autocorrelation consistent covariance matrix estimation. Econometrica 59, 817–854.

Astill, S., Harvey, D.I., Leybourne, S.J. and Taylor, A.M.R. (2017). Tests for an end-of-sample bubble in financial time series. Econometric Reviews 36, 651-666.

Bachelier, L. (1900). Théorie de la spéculation. Annales Scientifiques de l'Ecole Normale Supérieure, 3rd. 17:21–88. Translated in: The Random Character of Stock Market Prices, edited by Paul Cootner (1964), Cambridge.

Blanchard, O.J. and Watson, M.W. (1982). Bubbles, rational expectations, and financial markets. In P.Wachtel (ed.), Crisis in the Economic and Financial Structure, 295–315. Lexington: Lexington Books.

Breitung, J. and Kruse, R. (2013). When bubbles burst: econometric tests based on structural breaks. Statistical Papers 54, 911–930.

Campbell, J.Y. and R. Shiller (1989). The dividend-price ratio and expectations of future dividends and discount factors. Review of Financial Studies 1, 195–228.

Cavaliere, G. and Taylor, A.M.R. (2005). Stationarity tests under time-varying second moments. Econometric Theory 21, 1112–1129.

Cavaliere, G. and Taylor, A.M.R. (2008), Time-transformed unit root tests for models with non-stationary volatility. Journal of Time Series Analysis 29, 300–330.

Evans, G.W. (1991). Pitfalls in testing for explosive bubbles in asset prices. American Economic Review 81, 922-930.

Harvey, D.I., Leybourne, S.J. and Sollis, R. (2017). Improving the accuracy of asset price bubble start and end date estimators. Journal of Empirical Finance 40, 121-138.

Harvey, D.I., Leybourne, S.J. and Zu, Y. (2019). Testing explosive bubbles with time-varying volatility. Econometric Reviews 38, 1131-1151.

Harvey, D.I., Leybourne, S.J. and Zu, Y. (2020). Sign-based unit root tests for explosive financial bubbles in the presence of nonstationary volatility. Econometric Theory 36, 122-169.

Homm, U. and Breitung, J. (2012). Testing for speculative bubbles in stock markets: a comparison of alternative methods. Journal of Financial Econometrics 10, 198-231.

King, M.L. and G.H. Hillier (1985). Locally best invariant tests of the error covariance matrix of the linear regression model, Journal of the Royal Statistical Society, (Series B) 47, 98-102.

Kostakis, A., Magdalinos, T. and Stamatogiannis, M.P. (2015). Robust econometric inference for stock return predictability. Review of Financial Studies 28, 1506–1553.

Kwiatkowski, D., P.C.B. Phillips, P. Schmidt and Y. Shin (1992). Testing the null hypothesis of stationarity against the alternative of a unit root: how sure are we that economic time series have a unit root?, Journal of Econometrics 54, 159-178.

Nyblom, J. and T. Mäkeläinen (1983). Comparisons of tests for the presence of random walk coefficients in a simple linear model, Journal of the American Statistical Association 78, 856-864.

Phillips, P.C.B. and Shi, S.-P. (2018). Financial bubble implosion and reverse regression. Econometric Theory 34, 705-753.

Phillips, P.C.B., Shi, S.-P, and Yu, J. (2015). Testing for multiple bubbles: Historical episodes of exuberance and collapse in the S&P500. International Economic Review 56, 1043-1078.

Phillips, P.C.B., Wu, Y. and Yu, J. (2011). Explosive behavior in the 1990s Nasdaq: When did the exuberance escalate asset values? International Economic Review 52, 201-226.

Shi, S. and Phillips, P.C.B. (2023). Diagnosing housing fever with a econometric thermometer. Journal of Economic Surveys 37, 159–186.

Shorack, G.R. and Wellner, J.A. (1987). Empirical Processes and Their Applications to Statistics. New York: John Wiley and Sons.

Figure 1: Finite sample power of nominal 5% tests, $T = 200$, single bubble episode with $\tau_1 = 0.3$, $\tau_2 = 0.7$.

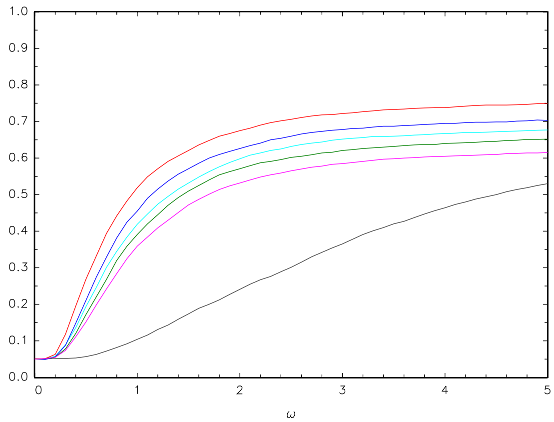

(a) $c = 1$, $GSADF$ and $S^*_{\bar{c}}$ tests

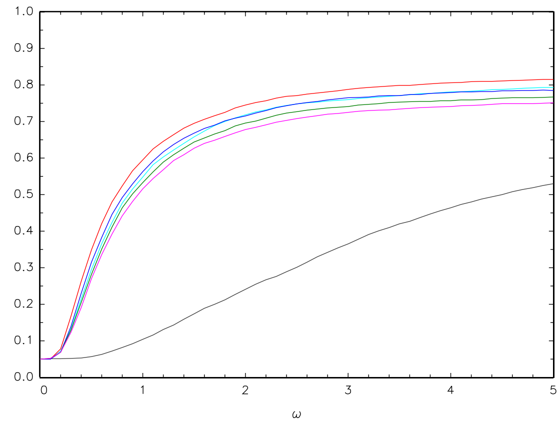

(b) $c = 1$, $GSADF$ and $S^\dagger_{\bar{c}}$ tests

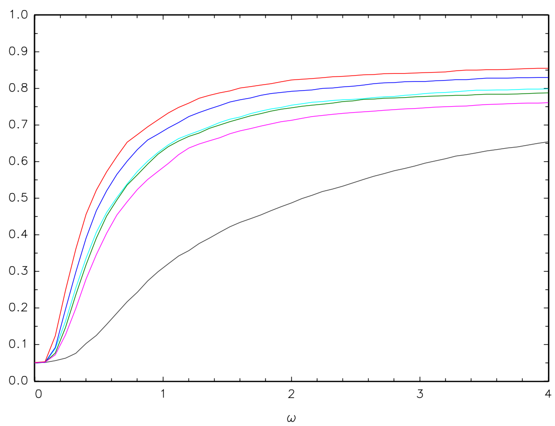

(c) $c = 2$, $GSADF$ and $S^*_{\bar{c}}$ tests

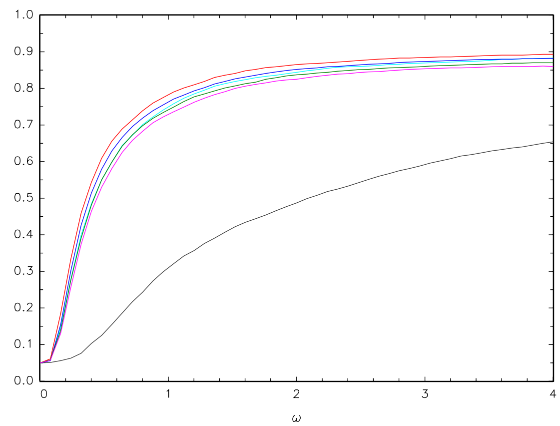

(d) $c = 2$, $GSADF$ and $S^\dagger_{\bar{c}}$ tests

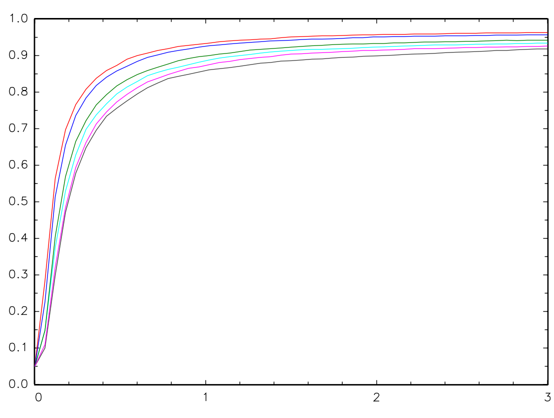

(e) $c = 4$, $GSADF$ and $S^*_{\bar{c}}$ tests

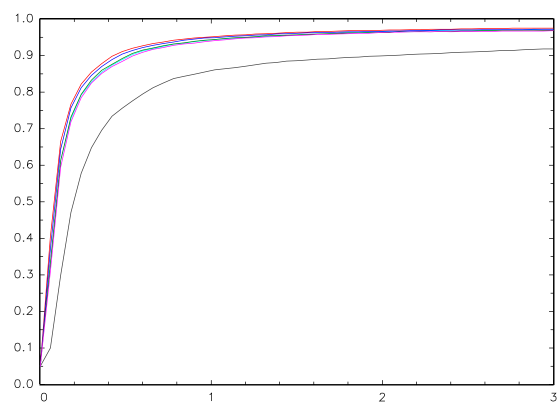

(f) $c = 4$, $GSADF$ and $S^\dagger_{\bar{c}}$ tests

$GSADF$: —— , $S^*_2, S^\dagger_2$: —— , $S^*_4, S^\dagger_4$: —— , $S^*_6, S^\dagger_6$: —— , $S^*_8, S^\dagger_8$: —— , $S^*_{10}, S^\dagger_{10}$: ——

Figure 2: Finite sample power of nominal 5% tests, $T = 200$, single bubble episode with $\tau_1 = 0.2$, $\tau_2 = 0.4$.

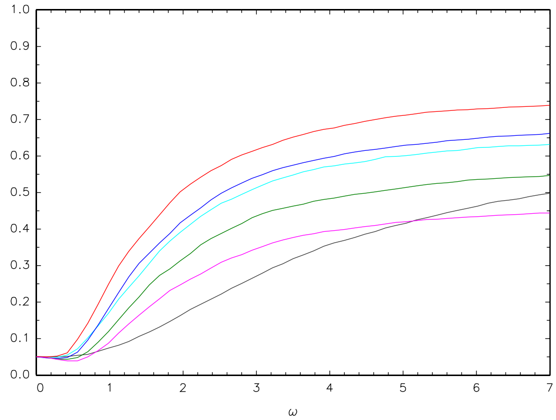

(a) $c = 0.5$, $GSADF$ and $S^*_{\bar{c}}$ tests

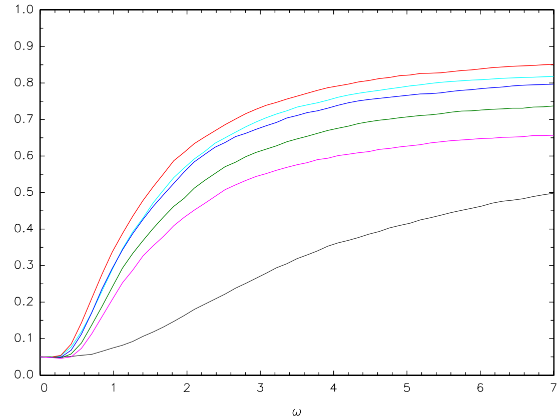

(b) $c = 0.5$, $GSADF$ and $S^\dagger_{\bar{c}}$ tests

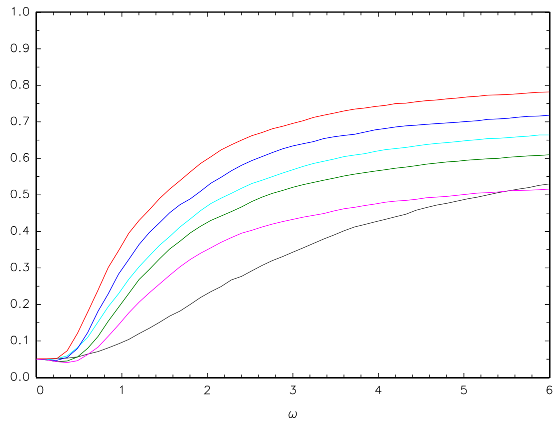

(c) $c = 1$, $GSADF$ and $S^*_{\bar{c}}$ tests

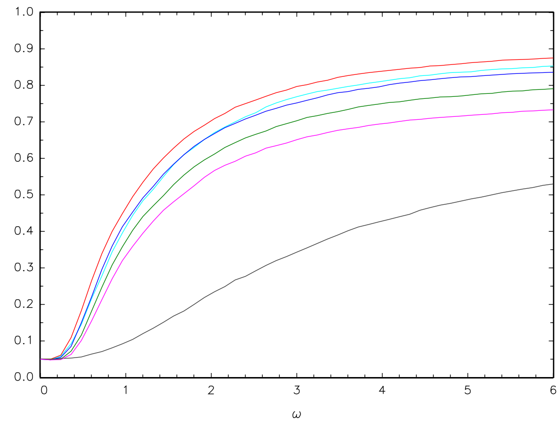

(d) $c = 1$, $GSADF$ and $S^\dagger_{\bar{c}}$ tests

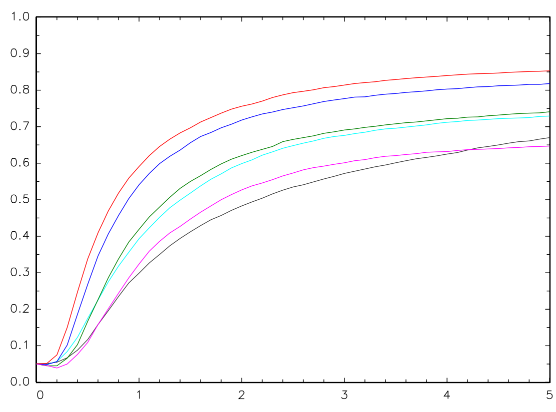

(e) $c = 2$, $GSADF$ and $S^*_{\bar{c}}$ tests

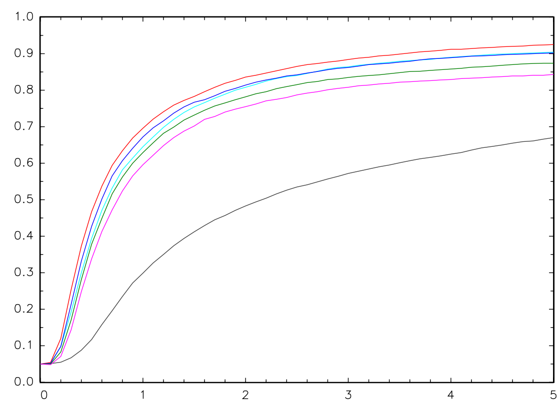

(f) $c = 2$, $GSADF$ and $S^\dagger_{\bar{c}}$ tests

$GSADF$: —— , $S^*_2, S^\dagger_2$: —— , $S^*_4, S^\dagger_4$: —— , $S^*_6, S^\dagger_6$: —— , $S^*_8, S^\dagger_8$: —— , $S^*_{10}, S^\dagger_{10}$: ——

Figure 3: Finite sample power of nominal 5% tests, $T = 200$, single bubble episode with $\tau_1 = 0.8$, $\tau_2 = 1$.

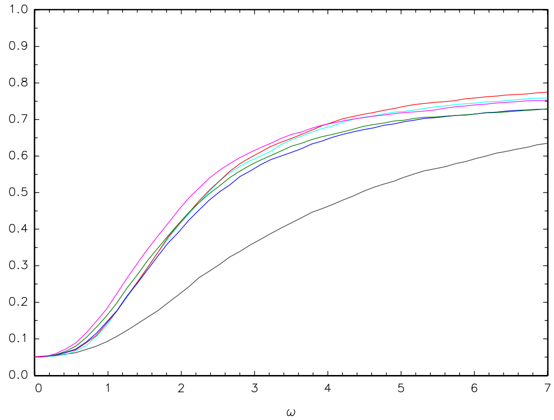

(a) $c = 0.5$, $GSADF$ and $S^*_{\bar{c}}$ tests

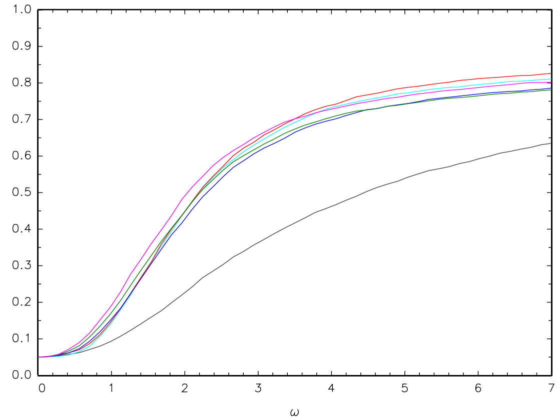

(b) $c = 0.5$, $GSADF$ and $S^\dagger_{\bar{c}}$ tests

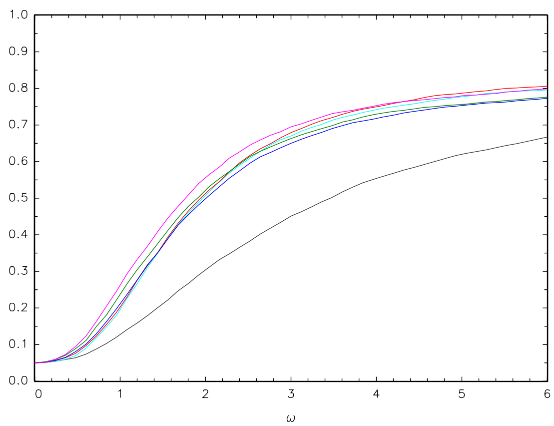

(c) $c = 1$, $GSADF$ and $S^*_{\bar{c}}$ tests

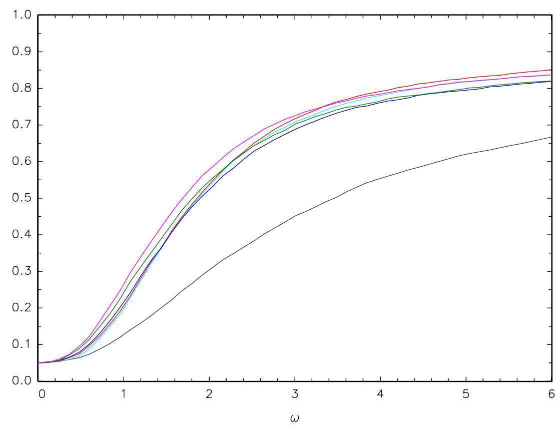

(d) $c = 1$, $GSADF$ and $S^\dagger_{\bar{c}}$ tests

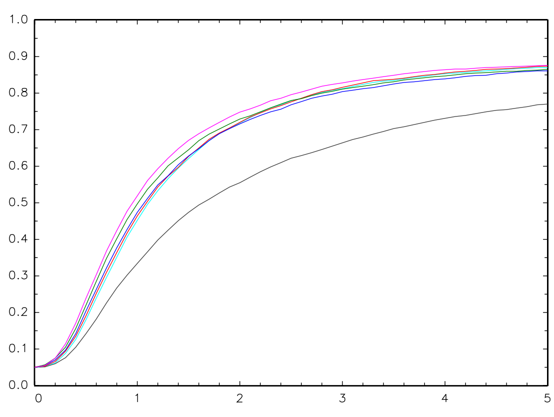

(e) $c = 2$, $GSADF$ and $S^*_{\bar{c}}$ tests

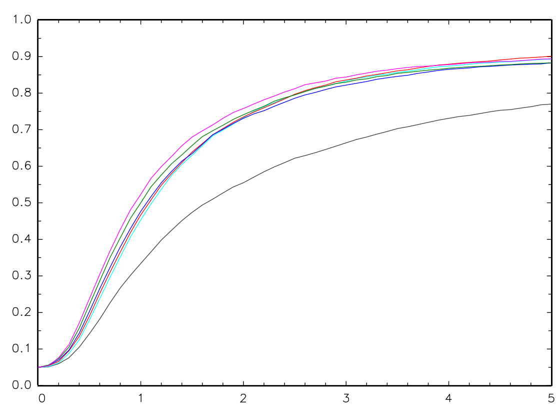

(f) $c = 2$, $GSADF$ and $S^\dagger_{\bar{c}}$ tests

$GSADF$: —, $S^*_2, S^\dagger_2$: —, $S^*_4, S^\dagger_4$: —, $S^*_6, S^\dagger_6$: —, $S^*_8, S^\dagger_8$: —, $S^*_{10}, S^\dagger_{10}$: —

Figure 4: Finite sample power of nominal 5% tests, $T = 200$, two bubble episodes with $\tau_{1,1} = 0.2$, $\tau_{2,1} = 0.4$ and $\tau_{1,2} = 0.6$, $\tau_{2,2} = 0.8$.

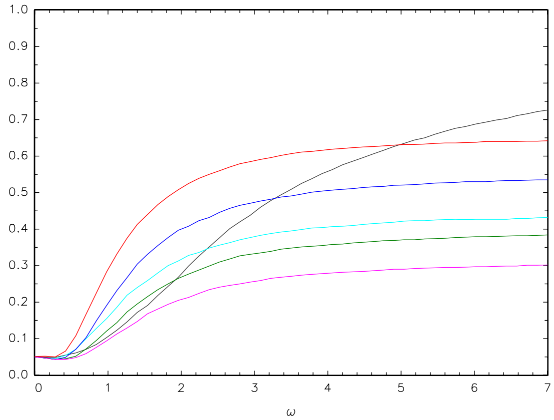

(a) $c = 0.5$, $GSADF$ and $S^*_{\bar{c}}$ tests

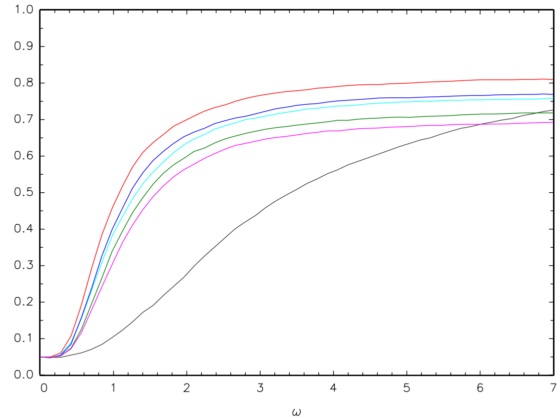

(b) $c = 0.5$, $GSADF$ and $S^\dagger_{\bar{c}}$ tests

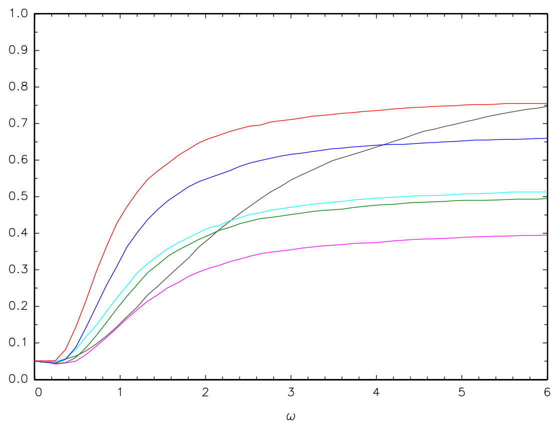

(c) $c = 1$, $GSADF$ and $S^*_{\bar{c}}$ tests

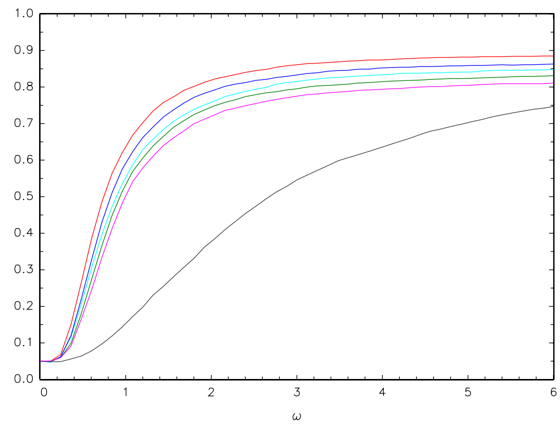

(d) $c = 1$, $GSADF$ and $S^\dagger_{\bar{c}}$ tests

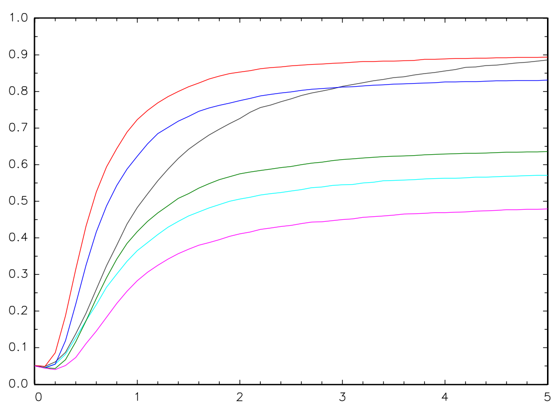

(e) $c = 2$, $GSADF$ and $S^*_{\bar{c}}$ tests

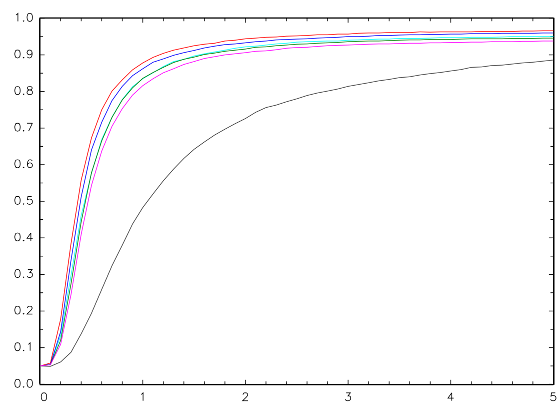

(f) $c = 2$, $GSADF$ and $S^\dagger_{\bar{c}}$ tests

$GSADF$: —— , $S^*_2, S^\dagger_2$: —— , $S^*_4, S^\dagger_4$: —— , $S^*_6, S^\dagger_6$: —— , $S^*_8, S^\dagger_8$: —— , $S^*_{10}, S^\dagger_{10}$: ——

Table 1: Finite Sample and Asymptotic 10%, 5% and 1% Critical Values for S_4^* and $S_4^\dagger$.

	10% level				5% level				1% level			
T	100	200	400	∞	100	200	400	∞	100	200	400	∞
S_4^*	8.538	8.759	8.917	9.066	8.686	8.880	9.033	9.182	8.966	9.131	9.248	9.399
$S_4^\dagger$, $k=1$	8.618	8.803	8.941	9.066	8.768	8.929	9.058	9.182	9.034	9.177	9.278	9.399
$S_4^\dagger$, $k=2$	8.687	8.843	8.962	9.066	8.843	8.970	9.080	9.182	9.102	9.214	9.299	9.399
$S_4^\dagger$, $k=3$	8.748	8.879	8.983	9.066	8.905	9.002	9.098	9.182	9.170	9.245	9.321	9.399

Table 2: Empirical Size of Nominal 5% Tests. DGP (10)–(12) under H_0 of (13) with $\varepsilon_t = \varphi\varepsilon_{t-1} + e_t$, $e_t \sim NIID(0,1)$.

Panel A: Short-Run Variance Estimate						
	$T=100$		$T=200$		$T=400$	
φ	S_4^*	$S_4^\dagger$	S_4^*	$S_4^\dagger$	S_4^*	$S_4^\dagger$
0.0	0.050	0.050	0.051	0.050	0.050	0.050
0.3	0.315	0.313	0.405	0.403	0.498	0.499
0.5	0.641	0.636	0.792	0.788	0.895	0.894
0.7	0.916	0.914	0.982	0.982	0.998	0.998
0.9	0.998	0.998	1.000	1.000	1.000	1.000
Panel B: Long-Run Variance Estimate						
	$T=100$		$T=200$		$T=400$	
φ	S_4^*	$S_4^\dagger$	S_4^*	$S_4^\dagger$	S_4^*	$S_4^\dagger$
0.0	0.045	0.048	0.049	0.047	0.045	0.047
0.3	0.056	0.074	0.047	0.056	0.046	0.051
0.5	0.051	0.073	0.042	0.050	0.036	0.044
0.7	0.056	0.074	0.034	0.047	0.026	0.030
0.9	0.128	0.123	0.056	0.058	0.030	0.035

Table 3: Empirical Application: Stationary Volatility and Bubble Detection Test Results

		Bootstrap p-values			
		Parametric		Wild	
Series	$\mathcal{H}_{AD}$	$S_4^{\dagger}$	$GSADF$	$S_4^{\dagger}$	$GSADF$
FTSE 100	3.517^{**}	0.019	0.206	0.084	0.468
DAX	3.950^{***}	0.001	0.002	0.012	0.114
CAC 40	1.953^{*}	0.003	0.110	0.014	0.314
Nikkei	0.187	0.200	0.043	0.174	0.110
NYSE Composite	3.626^{**}	0.023	0.453	0.060	0.658
S&P 500	4.697^{***}	0.025	0.417	0.076	0.704
Dow Jones Industrial Average	3.754^{**}	0.004	0.674	0.018	0.810
Nasdaq 100	8.926^{***}	0.004	0.055	0.076	0.262
Nasdaq Composite	8.799^{***}	0.023	0.061	0.136	0.346
Nasdaq Computer	7.652^{***}	0.027	0.128	0.128	0.370
Nasdaq Biotechnology	9.300^{***}	0.000	0.000	0.026	0.024
Nasdaq Telecommunications	10.558^{***}	0.003	0.048	0.058	0.300

Note: In the context of the stationary volatility tests, *, ** and *** denote rejection at the 10%, 5% and 1% nominal significance levels, respectively, based on the critical values from Table 5 of Shorack and Wellner (1987, p.148).

Supplementary Appendix to "An Unobserved Components Based Test for Asset Price Bubbles"

Sam Astill[a], David I. Harvey[b], Stephen J. Leybourne[b] and A.M. Robert Taylor[a]

[a] Essex Business School, University of Essex

[b] Granger Centre for Time Series Econometrics and School of Economics, University of Nottingham

November 28, 2025

Abstract

The contents of this supplementary appendix are as follows. In section A.1 we derive the scalar form representation of the LBI statistic, $S_\rho(\tau_{b1}, \tau_{b2})$, given in section 3.1. In section A.2 we detail the impact of unconditional heteroskedasticity on the tests from section 3 and develop a wild bootstrap implementation of our preferred test which recovers the first-order pivotal limiting null distribution in the presence of possible unconditional heteroskedasticity in the data. In section A.3 we provide proofs of the main theoretical results given in the paper, including those in section A.2, relating to the wild bootstrap test. Section A.4 provides details on the de-meaned variants of the tests that allow for a non-zero drift in the fundamental price. Material relating to the simulations for the univariate time-varying first-order autoregressive model discussed in section 5 of the paper is given in section A.5. Additional material relating to the empirical application is given in section A.6. Additional references cited in this supplementary appendix, but not in the main text, are then given after section A.6.

*We are grateful to participants at the opening conference of the Aarhus Center for Econometrics, May 2025, for helpful comments. Address correspondence to: Robert Taylor, Essex Business School, University of Essex, Wivenhoe Park, Colchester, CO4 3SQ, UK. Email: robert.taylor@essex.ac.uk.

A.1 Derivation of the Scalar Representation of the LBI statistic

The LBI statistic, $S_\rho(\tau_{b1}, \tau_{b2})$, with $t_{b1} = \lfloor \tau_{b1} T \rfloor$ and $t_{b2} = \lfloor \tau_{b2} T \rfloor$, takes the form

$$\begin{aligned} S_\rho(\tau_{b1}, \tau_{b2}) &= \frac{\boldsymbol{r}'\boldsymbol{MAM}'\boldsymbol{r}}{T^{-1}\boldsymbol{r}'\boldsymbol{r}} \\ &= \frac{\boldsymbol{r}'\boldsymbol{HH}'\boldsymbol{r}}{T^{-1}\boldsymbol{r}'\boldsymbol{r}} \end{aligned} \tag{A.1}$$

where $\boldsymbol{HH}'$ is the Cholesky decomposition of $\boldsymbol{MAM}'$ with $\boldsymbol{H}$ a $(T \times T)$ block diagonal lower triangular matrix which has (i, j)'th element $H_{i,j}$ equal to 0 for $i, j \notin [t_{b1}, ..., t_{b2}]$. For $i, j \in [t_{b1}, ..., t_{b2}]$ the $(i, j)'th$ element of $\boldsymbol{H}$ is given by

$$H_{i,j} = \begin{cases} 0 & i < j \\ 1 & i = j \\ (\rho - 1)\rho^{i-j-1} & i > j. \end{cases}$$

Expanding out the matrix products in (A.1), and after some algebra, we can rewrite $S_\rho(\tau_{b1}, \tau_{b2})$ in equivalent scalar form as

$$S_\rho(\tau_{b1}, \tau_{b2}) = \begin{cases} \dfrac{\left((\rho-1)\sum_{j=t_{b1}+1}^{t_{b2}} \rho^{j-t_{b1}-1}\Delta P_j\right)^2 + \sum_{t=t_{b1}+1}^{t_{b2}}\left(\Delta P_t + (\rho-1)\sum_{j=t+1}^{t_{b2}} \rho^{j-t-1}\Delta P_j\right)^2}{T^{-1}\sum_{t=2}^{T}(\Delta P_t)^2} & t_{b1} = 1 \\ \dfrac{\sum_{t=t_{b1}}^{t_{b2}}\left(\Delta P_t + (\rho-1)\sum_{j=t+1}^{t_{b2}} \rho^{j-t-1}\Delta P_j\right)^2}{T^{-1}\sum_{t=2}^{T}(\Delta P_t)^2} & t_{b1} > 1 \end{cases}$$

from which the form given in the main text follows immediately.

A.2 Allowing for Unconditional Heteroskedasticity

An important consideration in testing for an asset price bubbles is the potential for the innovations driving the price series to exhibit unconditional heteroskedasticity. While it is well established that for the financial time series on which bubbles tests are most often performed that conditional heteroskedasticity, such as GARCH behavior, is often present, several studies have also reported strong evidence of structural breaks in the unconditional variance of asset returns; see, among others, McMillan and Wohar (2011), Calvo-Gonzalez *et al.* (2010), and Vivian and Wohar (2012).

It is well known that it is difficult to discern between a series which contains a bubble and one which follows a unit process throughout but with heteroskedastic innovations, with many common tests for bubbles that are designed for homoskedastic innovations over-rejecting in the presence of the latter; see, for example Harvey *et al.* (2016). We therefore now examine how the presence of unconditional heteroskedasticity in ε_t and η_t impacts the limiting distribution of our proposed test statistics, and explore how a wild bootstrap implementation of the tests can deliver a testing strategy which maintains asymptotic size control.

To that end, we will replace Assumption 1 with the following assumption:

Assumption A.1. *Let $\varepsilon_t = \sigma_t z_{1t}$ and $\eta_t = \omega_t z_{2t}$ where z_{1t} and z_{2t} are independent MD sequences with unit variances and finite fourth order moments. The non-stochastic volatility sequences, σ_t and ω_t, satisfy $\sigma_t = \sigma(t/T)$ and $\omega_t = \omega(t/T)$, with $\sigma(\cdot) \in \mathcal{D}$ strictly positive and bounded and $\omega(\cdot) \in \mathcal{D}$ non-negative and bounded, where $\mathcal{D}$ denotes the space of right continuous with left limit (càdlàg) processes on $[0,1]$.*

In this heteroscedastic environment the null and alternative hypotheses can now represented by $H_0 : \omega(\cdot) = 0$ and $H_1 : \omega(\cdot) > 0$.

Under Assumption A.1, the limiting distributions of $S^*_{\bar{c}}$ and $S^\dagger_c$ are given in Theorem A.1.

Theorem A.1. *Let data be generated by (10)–(12). If Assumption A.1 holds then under H_1, as $T \to \infty$, we have that*

$$
\begin{aligned}
S^*_{\bar{c}} &\xrightarrow{w} \sup_{\tau_1 \in [0,1-\pi]} \sup_{\tau_2 \in [\tau_1+\pi,1]} \log H_{c,\bar{c}}(\tau_1, \tau_2, \omega(\cdot), \sigma(\cdot), \tau_{b1}, \tau_{b2}), \\
S^\dagger_c &\xrightarrow{w} \sup_{\tau_1 \in [0,1-\pi]} \sup_{\tau_2 \in [\tau_1+\pi,1]} \log G_{c,\bar{c}}(\tau_1, \tau_2, \omega(\cdot), \sigma(\cdot), \tau_{b1}, \tau_{b2})
\end{aligned}
$$

where

$$H_{c,\bar{c}}(\tau_1,\tau_2,\omega(\cdot),\sigma(\cdot),\tau_{b1},\tau_{b2}) := \frac{N_{c,\bar{c}}(\tau_1,\tau_2,\omega(\cdot),\sigma(\cdot),\tau_{b1},\tau_{b2})}{\int_0^1 \sigma(r)^2 dr + \int_{\tau_{b1}}^{\tau_{b2}} \omega(r)^2 dr + \left\{\int_{\tau_{b1}}^{\tau_{b2}} e^{c(\tau_{b2}-s)(\tau_{b2}-\tau_{b1})^{-1}} \omega(s) dW_\eta(s)\right\}^2}$$

$$G_{c,\bar{c}}(\tau_1,\tau_2,\omega(\cdot),\sigma(\cdot),\tau_{b1},\tau_{b2}) := \frac{N_{c,\bar{c}}(\tau_1,\tau_2,\omega(\cdot),\sigma(\cdot),\tau_{b1},\tau_{b2})}{\int_0^1 \sigma(r)^2 dr + \int_{\tau_{b1}}^{\tau_{b2}} \omega(r)^2 dr}$$

with

$$N_{c,\bar{c}}(\tau_1,\tau_2,\omega(\cdot),\sigma(\cdot),\tau_{b1},\tau_{b2}) := \bar{c}^2(\tau_2-\tau_1)^{-2} \int_{\tau_1}^{\tau_2} \left\{\int_r^{\tau_2} e^{\bar{c}(s-r)(\tau_2-\tau_1)^{-1}} dK_c(s,\omega(\cdot),\sigma(\cdot),\tau_{b1},\tau_{b2})\right\}^2 dr$$

and

$$K_c(r,\omega(\cdot),\sigma(\cdot),\tau_{b1},\tau_{b2}) := \int_0^r \sigma(s) dW_\varepsilon(s) + \mathbb{I}(\tau_{b1} \le r \le \tau_{b2}) \int_{\tau_{b1}}^r e^{c(r-s)(\tau_{b2}-\tau_{b1})^{-1}} \omega(s) dW_\eta(s)$$

where $W_\varepsilon(r)$ and $W_\eta(r)$ are independent standard Brownian motions.

Remark A.2.1. Notice from Theorem A.1 that the limiting null distributions of $S_{\bar{c}}^*$ and $S_c^\dagger$ are given by $H_{c,\bar{c}}(\tau_1,\tau_2,0,\sigma(\cdot),\tau_{b1},\tau_{b2})$ and $G_{c,\bar{c}}(\tau_1,\tau_2,0,\sigma(\cdot),\tau_{b1},\tau_{b2})$ which coincide and can be denoted more simply as $H_{\bar{c}}(\tau_1,\tau_2,\sigma(\cdot))$ and $G_{\bar{c}}(\tau_1,\tau_2,\sigma(\cdot))$, since they do not depend on c, τ_{b1} or τ_{b2}. Clearly then, heteroskedasticity in ε_t introduces nuisance parameters into the limiting null distributions of the $S_{\bar{c}}^*$ and $S_c^\dagger$ statistics, such that the homoskedastic critical values given in Table 1 will no longer be appropriate. Notice also that in the homoskedastic null case $H_{\bar{c}}(\tau_1,\tau_2,1) = G_{\bar{c}}(\tau_1,\tau_2,1) = L_{\bar{c}}(\tau_1,\tau_2)$. ◊

Remark A.2.2. It is also seen from the representations in Theorem A.1 that the asymptotic local power functions of the tests based on $S_{\bar{c}}^*$ and $S_c^\dagger$ will differ from one another, as in the homoskedastic case, and will also both depend on nuisance parameters arising from any heteroskedasticity present in ε_t and η_t. ◊

A.2.1 Wild Bootstrap Implementation

Theorem A.1 shows that the limiting distributions of the $S^*_{\bar{c}}$ and $S^\dagger_{\bar{c}}$ test statistics under heteroskedasticity of the form given by Assumption A.1 are different from those that obtain under homoskedasticity, as specified by Assumption 1. To address the inference problem this causes, we now outline a wild bootstrap algorithm that can be used to generate asymptotically valid bootstrap critical values and p-values for the tests based on the $S^*_{\bar{c}}$ and $S^\dagger_{\bar{c}}$ statistics, allowing us to implement tests with asymptotic size control in the presence of heteroskedasticity of the form given in Assumption A.1. We outline the procedure for the $S^\dagger_{\bar{c}}$ test, but the algorithm could equally be used for the $S^*_{\bar{c}}$ test.

Algorithm A.1. ***(Wild Bootstrap for the $S^\dagger_{\bar{c}}$ test)***

Step 1: *Compute the $S^\dagger_{\bar{c}}$ test statistic as in (18).*

Step 2: *Generate $\Delta P^b_t := w_t \Delta P_t$, $t = 2, ..., T$, where w_t denotes an $NIID(0,1)$ sequence.*

Step 3: *Construct the bootstrap statistic*

$$S^b_{\bar{c}} := \sup_{\tau_1 \in [1/T, 1-\pi]} \sup_{\tau_2 \in [\tau_1+\pi, 1]} \log S^b_{\bar{c}}(\tau_1, \tau_2)$$

where

$$S^b_{\bar{c}}(\tau_1, \tau_2) := \frac{\bar{c}^2 (t_2 - t_1)^{-2} \sum_{t=t_1+1}^{t_2} \left(\sum_{j=t}^{t_2} \{1 + \bar{c}(t_2 - t_1)^{-1}\}^{j-t} \Delta P^b_j \right)^2}{\hat{\sigma}^2} \tag{A.2}$$

Step 4: *Repeat steps 2-3 B times and compute bootstrap critical values from the sequence of bootstrap statistics $S^b_{\bar{c}}$, $b = 1, ..., B$.*

Step 5: *To perform a test at the α level of significance, compare the test statistic $S^\dagger_{\bar{c}}$ from Step 1 to the $(1-\alpha)$ quantile of the $S^b_{\bar{c}}$ test statistics, $b = 1, ..., B$. Alternatively, a p-value for the test can be computed as $p(S^\dagger_{\bar{c}}) := B^{-1} \sum_{i=1}^{B} \mathbb{I}(S^b_{\bar{c}} > S^\dagger_{\bar{c}})$.*

Remark A.2.3. Note that we do not need to employ bootstrap data in the denominator of the bootstrap statistic (A.2), and we found superior finite sample performance was obtained when using $\hat{\sigma}^2$ rather than its equivalent based on the bootstrap data. Moreover we use $\hat{\sigma}^2$ (as in $S_{\bar{c}}^*$) rather than $\hat{\sigma}_m^2$ (as in $S_{\bar{c}}^\dagger$) here. This is because, other things equal, under the alternative we want the bootstrap quantiles to be as small as possible in order to maximize power, and using $\hat{\sigma}^2$ results in a larger denominator in the bootstrap statistics than using $\hat{\sigma}_m^2$. $\diamondsuit$

Remark A.2.4. To improve the finite sample performance of the bootstrap test, in the sub-sample statistics underlying the $S_{\bar{c}}^b$ statistic, we calculate the numerator while removing the largest absolute value of ΔP_t^b. This modification has no impact on the asymptotic properties of the bootstrap statistic under the null, but might be expected to lead to a reduction in the magnitude of the bootstrap statistic under the alternative, and thereby potentially improve power. $\diamondsuit$

In Theorem A.2 we next establish the limiting distribution of the bootstrap statistic $S_{\bar{c}}^b$ from Algorithm A.1 under Assumption A.1.

Theorem A.2. *Let the data be generated by (10)–(12). If Assumption A.1 holds then under H_1, as $T \to \infty$, we have that*

$$S_{\bar{c}}^b \xrightarrow{w}_p \sup_{\tau_1 \in [0,1-\pi]} \sup_{\tau_2 \in [\tau_1+\pi,1]} \log H_{0,\bar{c}}(\tau_1, \tau_2, \omega(\cdot), \sigma(\cdot), \tau_{b1}, \tau_{b2})$$

where '$\xrightarrow{w}_p$' denotes weak convergence in probability, and where

$$H_{0,\bar{c}}(\tau_1, \tau_2, \omega(\cdot), \sigma(\cdot), \tau_{b1}, \tau_{b2}) := \frac{N_{0,\bar{c}}(\tau_1, \tau_2, \omega(\cdot), \sigma(\cdot), \tau_{b1}, \tau_{b2})}{\int_0^1 \sigma(r)^2 dr + \int_{\tau_{b1}}^{\tau_{b2}} \omega(r)^2 dr + \left\{ \int_{\tau_{b1}}^{\tau_{b2}} e^{c(\tau_{b2}-s)(\tau_{b2}-\tau_{b1})^{-1}} \omega(s) dW_\eta(s) \right\}^2}$$

Remark A.2.5. The asymptotic null distribution of the $S_{\bar{c}}^b$ statistic is therefore given by $H_{\bar{c}}(\tau_1, \tau_2, \sigma(\cdot)) = G_{\bar{c}}(\tau_1, \tau_2, \sigma(\cdot))$. This is seen to be the same limiting null distribution, to first order, as that of $S_{\bar{c}}^*$ and $S_{\bar{c}}^\dagger$, discussed in Remark A.2.1. Comparing the $S_{\bar{c}}^\dagger$ statistic to its bootstrap critical value generated from Algorithm A.1 will therefore yield tests with asymptotically controlled size. $\diamondsuit$

Remark A.2.6. Ideally, under the alternative we would like $H_{0,\bar{c}}(\tau_1, \tau_2, \omega(\cdot), \sigma(\cdot), \tau_{b1}, \tau_{b2})$ to coincide with $H_{\bar{c}}(\tau_1, \tau_2, \sigma(\cdot))$ from Theorem A.1, but this can be seen not to be the case. The numerator of $H_{0,\bar{c}}(\tau_1, \tau_2, \omega(\cdot), \sigma(\cdot), \tau_{b1}, \tau_{b2})$ does not, however, depend on c and so a test based on bootstrap critical values would still be expected to retain good power properties. ◇

Remark A.2.7. In the case of weakly dependent errors, $S_{\bar{c}}^{\dagger}$ is constructed using a long run variance estimator but no additional changes are required in the bootstrap algorithm. ◇

A.2.2 Wild Bootstrap Finite Sample Simulations

We next report results of a small Monte Carlo simulation exercise examining the ability of the wild bootstrap implementation of the $S_{\bar{c}}^{\dagger}$ test to control size when the innovations to the fundamental price series in (11), ε_t, exhibit time-varying volatility. Data are generated according to (10)–(12) with $T = 200$, $\varepsilon_t \sim NIID(0, \sigma_t^2)$, $\eta_t \sim NIID(0, \omega^2)$ and $\rho = 1 + c(t_{b2} - t_{b1})^{-1}$ with $c = 2$, where the start and end dates of the bubble are given by $t_{b1} = \lfloor \tau_{b1} T \rfloor$ and $t_{b2} = \lfloor \tau_{b2} T \rfloor$, respectively, with $\tau_{b1} = 0.3$ and $\tau_{b2} = 0.7$. We specify the following function for σ_t,

$$\sigma_t := \begin{cases} \sigma & t = \lfloor 0.3T \rfloor, ..., \lfloor 0.7T \rfloor \\ 1 & \text{otherwise} \end{cases} \tag{A.3}$$

The timings of the potential volatility shifts are therefore chosen to match the start and end dates of the (potential) bubble episode. When $\sigma = 1$ the innovations ε_t are unconditionally homoskedastic whereas when $\sigma > 1$ ($\sigma < 1$) the innovations are subject to an upward (downward) shift in volatility from 1 to σ, before the volatility subsequently falls (increases) back to 1.

We report results based on 2000 Monte Carlo replications for our preferred $S_4^{\dagger}$ test (again setting $\pi = 0.1$ and removing the single largest absolute value of ΔP_t in calculating the variance estimate) compared to finite 5% level finite sample critical values and when compared to 5% level wild bootstrap critical values based on 500 bootstrap replications obtained using the wild bootstrap outlined in Algorithm A.1, together with the adjustment discussed in Remark A.2.4.

We begin by examining the size of the tests when $\omega = 0$, with results reported for $\sigma \in \{1, 1/2, 1/3, 2, 3\}$ in Table A.1. From these results we observe that when $\sigma = 1$, such that the series is unconditionally homoskedastic, both the non-bootstrap $S_4^\dagger$ test, and the corresponding bootstrap $S_4^\dagger$ test, have approximately correct size. When $\sigma \neq 1$, such that a volatility shift occurs, we see that, as expected, the $S_4^\dagger$ test based on finite sample (homoskedastic) critical values suffers from considerable upward size distortions. The bootstrap $S_4^{\dagger b}$ test shows much smaller size distortions than the $S_4^\dagger$ test based on homoskedastic critical values, but is still rather oversized, the more so for $\sigma > 1$ *vis-à-vis* $\sigma < 1$.

Table A.1: Empirical Size and Power of Nominal 5% Tests with Non-Stationary Volatility

	$\omega = 0$		$\omega = 1$	
σ	$S_4^\dagger$	Bootstrap $S_4^\dagger$	$S_4^\dagger$	Bootstrap $S_4^\dagger$
1	0.049	0.044	0.762	0.757
1/2	0.124	0.064	0.782	0.792
1/3	0.177	0.067	0.787	0.801
2	0.252	0.082	0.747	0.668
3	0.374	0.094	0.729	0.582

We next examine the the power of the tests when $\omega = 2$, with these results also reported in Table A.1. We can ignore the power of the non-bootstrap $S_4^\dagger$ test in all but the homoskedastic case because of its size distortions. The bootstrap $S_4^\dagger$ test is seen to display reasonably good power across all values of σ and, notably, loses relatively little power compared to its non-bootstrap counterpart in the homoskedastic case.

A.3 Proofs

Proof of Theorem 1

First we obtain the behavior of the partial sum process for ΔP_t:

$$\begin{aligned}
T^{-1/2}\sum_{t=2}^{\lfloor rT\rfloor}\Delta P_t &= T^{-1/2}P_{\lfloor rT\rfloor} - T^{-1/2}P_1 \\
&= T^{-1/2}P_{\lfloor rT\rfloor} + o_p(1) \\
&= T^{-1/2}F_{\lfloor rT\rfloor} + \begin{cases} T^{-1/2}[\{1+c(t_{b2}-t_{b1})^{-1}\}B_{\lfloor rT\rfloor-1}+\eta_{\lfloor rT\rfloor}] + o_p(1) & t = t_{b1},...,t_{b2} \\ o_p(1) & \text{otherwise} \end{cases} \\
&= T^{-1/2}F_{\lfloor rT\rfloor} + \begin{cases} T^{-1/2}\{e^{c(t_{b2}-t_{b1})^{-1}}B_{\lfloor rT\rfloor-1}+\eta_{\lfloor rT\rfloor}\} + o_p(1) & t = t_{b1},...,t_{b2} \\ o_p(1) & \text{otherwise} \end{cases} \\
&\xrightarrow{w} \sigma W_\varepsilon(r) + \mathbb{I}(\tau_{b1}\le r\le \tau_{b2})\omega\int_{\tau_{b1}}^{r} e^{c(r-s)(\tau_{b2}-\tau_{b1})^{-1}}dW_\eta(s) \\
&=: \sigma K_c(r,\omega/\sigma,\tau_{b1},\tau_{b2}).
\end{aligned}$$

Next,

$$T^{-1/2}\sum_{j=t}^{t_2}\{1+\bar{c}(t_2-t_1)^{-1}\}^{j-t}\Delta P_j = T^{-1/2}\sum_{j=t}^{t_2}\{e^{\bar{c}(t_2-t_1)^{-1}}\}^{j-t}\Delta P_j + o_p(1).$$

Then,

$$T^{-1/2}\sum_{j=\lfloor rT\rfloor}^{\lfloor \tau_2 T\rfloor}\{e^{\bar{c}(\lfloor\tau_2 T\rfloor-\lfloor\tau_1 T\rfloor)^{-1}}\}^{j-\lfloor rT\rfloor}\Delta P_j \xrightarrow{w} \sigma\int_r^{\tau_2} e^{\bar{c}(s-r)(\tau_2-\tau_1)^{-1}}dK_c(s,\omega/\sigma,\tau_{b1},\tau_{b2})$$

and, hence,

$$
\begin{aligned}
&\bar{c}^2(t_2-t_1)^{-2}\sum_{t=t_1+1}^{t_2}\left(\sum_{j=t}^{t_2}\{1+\bar{c}(t_2-t_1)^{-1}\}^{j-t}\Delta P_j\right)^2 \\
&\qquad = \bar{c}^2(\tau_2-\tau_1)^{-2}T^{-1}\sum_{t=t_1+1}^{t_2}\left(T^{-1/2}\sum_{j=t}^{t_2}\{1+\bar{c}(t_2-t_1)^{-1}\}^{j-t}P_j\right)^2 \\
&\qquad \xrightarrow{w} \bar{c}^2(\tau_2-\tau_1)^{-2}\sigma^2\int_{\tau_1}^{\tau_2}\left\{\int_r^{\tau_2}e^{\bar{c}(s-r)(\tau_2-\tau_1)^{-1}}dK_c(s,\omega/\sigma,\tau_{b1},\tau_{b2})\right\}^2 dr.
\end{aligned}
$$

Next,

$$
T^{-1}\sum_{t=2}^{T}(\Delta P_t)^2 = T^{-1}\sum_{t=2}^{t_{b1}-1}(\Delta P_t)^2 + T^{-1}\sum_{t=t_{b1}}^{t_{b2}}(\Delta P_t)^2 + T^{-1}(\Delta P_{t_{b2}+1})^2 + T^{-1}\sum_{t=t_{b2}+2}^{T}(\Delta P_t)^2.
$$

Here, straightforwardly, $T^{-1}\sum_{t=2}^{t_{b1}-1}(\Delta P_t)^2 = \tau_{b1}\sigma^2 + o_p(1)$ and $T^{-1}\sum_{t=t_{b2}+2}^{T}(\Delta P_t)^2 = (1-\tau_{b2})\sigma^2 + o_p(1)$. Also

$$
T^{-1}\sum_{t=t_{b1}}^{t_{b2}}(\Delta P_t)^2 = (\tau_{b2}-\tau_{b1})(\sigma^2+\omega^2) + o_p(1)
$$

owing to the fact that ε_t and η_t are uncorrelated. For the remaining term,

$$
\begin{aligned}
T^{-1}(\Delta P_{t_{b2}+1})^2 &= T^{-1}(-B_{t_{b2}})^2 + o_p(1) \\
&= (T^{-1/2}B_{\lfloor \tau_{b2}T\rfloor})^2 + o_p(1) \\
&= [T^{-1/2}\{e^{c(t_{b2}-t_{b1})^{-1}}B_{\lfloor \tau_{b2}T\rfloor -1} + \eta_{\lfloor \tau_{b2}T\rfloor}\}]^2 + o_p(1) \\
&\xrightarrow{w} \omega^2\left\{\int_{\tau_{b1}}^{\tau_{b2}} e^{c(\tau_{b2}-s)(\tau_{b2}-\tau_{b1})^{-1}}dW_\eta(s)\right\}^2.
\end{aligned}
$$

Consequently,

$$
\begin{aligned}
T^{-1}\sum_{t=2}^{T}(\Delta P_t)^2 &\xrightarrow{w} \sigma^2 + \omega^2(\tau_{b2}-\tau_{b1}) + \omega^2\left\{\int_{\tau_{b1}}^{\tau_{b2}} e^{c(\tau_{b2}-s)(\tau_{b2}-\tau_{b1})^{-1}}dW_\eta(s)\right\}^2 \\
&= \sigma^2\left[1+\left(\frac{\omega}{\sigma}\right)^2(\tau_{b2}-\tau_{b1}) + \left(\frac{\omega}{\sigma}\right)^2\left\{\int_{\tau_{b1}}^{\tau_{b2}} e^{c(\tau_{b2}-s)(\tau_{b2}-\tau_{b1})^{-1}}dW_\eta(s)\right\}^2\right].
\end{aligned}
$$

Finally, collecting these results together we have that,

$$\begin{aligned} S_{\bar{c}}^{*}(\tau_1,\tau_2) &\overset{w}{\to} \frac{\bar{c}^2(\tau_2-\tau_1)^{-2}\int_{\tau_1}^{\tau_2}\left\{\int_r^{\tau_2} e^{\bar{c}(s-r)(\tau_2-\tau_1)^{-1}} dK_c(s,\omega/\sigma,\tau_{b1},\tau_{b2})\right\}^2 dr}{1+\left(\frac{\omega}{\sigma}\right)^2(\tau_{b2}-\tau_{b1})+\left(\frac{\omega}{\sigma}\right)^2\left\{\int_{\tau_{b1}}^{\tau_{b2}} e^{c(\tau_{b2}-s)(\tau_{b2}-\tau_{b1})^{-1}} dW_\eta(s)\right\}^2} \\ &=: H_{c,\bar{c}}(\tau_1,\tau_2,\omega/\sigma,\tau_{b1},\tau_{b2}) \end{aligned} \tag{A.4}$$

The large sample result in (A.4) holds formally only for fixed τ_1, τ_2. However, following the same approach (which is based on the proof strategy adopted by Zivot and Andrews, 1992, to prove their Theorem 1) as that used to establish Equation (A.6) on p.1072 in the proof of Theorem 1 in PSY (pp.1072-1075), the stated result for the limiting distribution of the $S_{\bar{c}}^{*}$ statistic can be shown to follow by means of the Continuous Mapping Theorem (CMT) from the fixed τ_1, τ_2 representation in (A.4).

Proof of Theorem A.1

First note that

$$\begin{aligned} T^{-1/2}\sum_{t=1}^{\lfloor rT\rfloor}\varepsilon_t &\overset{w}{\to} \int_0^r \sigma(s)dW_\varepsilon(s), \\ T^{-1/2}\sum_{t=1}^{\lfloor rT\rfloor}\eta_t &\overset{w}{\to} \int_0^r \omega(s)dW_\eta(s). \end{aligned}$$

Then we obtain the behavior of the partial sum process for ΔP_t as

$$\begin{aligned} T^{-1/2}\sum_{t=2}^{\lfloor rT\rfloor}\Delta P_t &\overset{w}{\to} \int_0^r \sigma(s)dW_\varepsilon(s)+\mathbb{I}(\tau_{b1}\le r\le\tau_{b2})\int_{\tau_{b1}}^r e^{c(r-s)(\tau_{b2}-\tau_{b1})^{-1}}\omega(s)dW_\eta(s) \\ &=: K_c(r,\omega(\cdot),\sigma(\cdot),\tau_{b1},\tau_{b2}). \end{aligned}$$

Hence,

$$\bar{c}^2(t_2-t_1)^{-2}\sum_{t=t_1+1}^{t_2}\left(\sum_{j=t}^{t_2}\{1+\bar{c}(t_2-t_1)^{-1}\}^{j-t}\Delta P_j\right)^2$$

$$\begin{aligned} &= \bar{c}^2(\tau_2-\tau_1)^{-2}T^{-1}\sum_{t=t_1+1}^{t_2}\left(T^{-1/2}\sum_{j=t}^{t_2}\{1+\bar{c}(t_2-t_1)^{-1}\}^{j-t}\Delta P_j\right)^2 \\ &\xrightarrow{w} \bar{c}^2(\tau_2-\tau_1)^{-2}\int_{\tau_1}^{\tau_2}\left\{\int_r^{\tau_2} e^{\bar{c}(s-r)(\tau_2-\tau_1)^{-1}}dK_c(s,\omega(\cdot),\sigma(\cdot),\tau_{b1},\tau_{b2})\right\}^2 dr. \end{aligned}$$

Next,

$$T^{-1}\sum_{t=2}^{T}(\Delta P_t)^2 = T^{-1}\sum_{t=2}^{t_{b1}-1}(\Delta P_t)^2 + T^{-1}\sum_{t=t_{b1}}^{t_{b2}}(\Delta P_t)^2 + T^{-1}(\Delta P_{t_{b2}+1})^2 + T^{-1}\sum_{t=t_{b2}+2}^{T}(\Delta P_t)^2$$

Here, $T^{-1}\sum_{t=2}^{t_{b1}-1}(\Delta P_t)^2 = \int_0^{\tau_{b1}}\sigma(r)^2dr + o_p(1)$ and $T^{-1}\sum_{t=t_{b2}+2}^{T}(\Delta P_t)^2 = \int_{\tau_{b2}}^1\sigma(r)^2dr$ $+o_p(1)$. Also

$$T^{-1}\sum_{t=t_{b1}}^{t_{b2}}(\Delta P_t)^2 = \int_{\tau_{b1}}^{\tau_{b2}}\{\sigma(r)^2+\omega^2(r)\}dr + o_p(1).$$

For the remaining term,

$$T^{-1}(\Delta P_{t_{b2}+1})^2 \xrightarrow{w} \left\{\int_{\tau_{b1}}^{\tau_{b2}} e^{c(\tau_{b2}-s)(\tau_{b2}-\tau_{b1})^{-1}}\omega(s)dW_\eta(s)\right\}^2.$$

So, in total,

$$T^{-1}\sum_{t=2}^{T}(\Delta P_t)^2 \xrightarrow{w} \int_0^1\sigma(r)^2dr + \int_{\tau_{b1}}^{\tau_{b2}}\omega(r)^2dr + \left\{\int_{\tau_{b1}}^{\tau_{b2}} e^{c(\tau_{b2}-s)(\tau_{b2}-\tau_{b1})^{-1}}\omega(s)dW_\eta(s)\right\}^2.$$

Finally, collecting these results together we have that

$$\begin{aligned} S^*_{\bar{c}}(\tau_1,\tau_2) &\xrightarrow{w} \frac{\bar{c}^2(\tau_2-\tau_1)^{-2}\int_{\tau_1}^{\tau_2}\left\{\int_r^{\tau_2} e^{\bar{c}(s-r)(\tau_2-\tau_1)^{-1}}dK_c(s,\omega(\cdot),\sigma(\cdot),\tau_{b1},\tau_{b2})\right\}^2 dr}{\int_0^1\sigma(r)^2dr + \int_{\tau_{b1}}^{\tau_{b2}}\omega(r)^2dr + \left\{\int_{\tau_{b1}}^{\tau_{b2}} e^{c(\tau_{b2}-s)(\tau_{b2}-\tau_{b1})^{-1}}\omega(s)dW_\eta(s)\right\}^2} \\ &=: H_{c,\bar{c}}(\tau_1,\tau_2,\omega(\cdot),\sigma(\cdot),\tau_{b1},\tau_{b2}). \end{aligned} \tag{A.5}$$

The stated limiting distribution for the $S^*_{\bar{c}}$ statistic then follows from the fixed τ_1, τ_2 representation in (A.5) using the CMT by the same arguments as are made at the end of the proof of Theorem 1. The limiting distribution of the $S_{\bar{c}}^{\dagger}$ statistic then follows trivially from that of the $S_{\bar{c}}^{*}$ statistic.

Proof of Theorem A.2

Here

$$\begin{aligned}
& T^{-1/2}\sum_{t=2}^{\lfloor rT \rfloor} \Delta P_t^b \\
= \; & T^{-1/2}\sum_{t=2}^{\lfloor rT \rfloor} w_t \Delta P_t \\
= \; & T^{-1/2}\sum_{t=2}^{\lfloor rT \rfloor} w_t \varepsilon_t + \begin{cases} T^{-1/2}c(t_{b2}-t_{b1})^{-1}\sum_{t=2}^{\lfloor rT \rfloor} w_t F_{t-1} + T^{-1/2}\sum_{t=2}^{\lfloor rT \rfloor} w_t \eta_t & t = t_{b1},...,t_{b2} \\ 0 & \text{otherwise} \end{cases} + o_p(1).
\end{aligned}$$

Now,

$$\begin{aligned}
T^{-1/2}c(t_{b2}-t_{b1})^{-1}\sum_{t=2}^{\lfloor rT \rfloor} w_t F_{t-1} &= cT^{1/2}(t_{b2}-t_{b1})^{-1}T^{-1}\sum_{t=2}^{\lfloor rT \rfloor} w_t F_{t-1} \\
&= O(T^{-1/2}) \times O_p(1) = O_p(T^{-1/2}),
\end{aligned}$$

and so

$$\begin{aligned}
T^{-1/2}\sum_{t=2}^{\lfloor rT \rfloor} \Delta P_t^b &= T^{-1/2}\sum_{t=2}^{\lfloor rT \rfloor} w_t \varepsilon_t + \begin{cases} T^{-1/2}\sum_{t=2}^{\lfloor rT \rfloor} w_t \eta_t & t = t_{b1},...,t_{b2} \\ 0 & \text{otherwise} \end{cases} + o_p(1) \\
&\xrightarrow{w}_p \int_0^r \sigma(s)dW_\varepsilon(s) + \mathbb{I}(\tau_{b1} \le r \le \tau_{b2})\int_{\tau_{b1}}^r \omega(s)dW_\eta(s) \\
&= K_0(r, \omega(\cdot), \sigma(\cdot), \tau_{b1}, \tau_{b2}).
\end{aligned}$$

Next,

$$
\begin{aligned}
T^{-1}\sum_{t=2}^{T}(\Delta P_t^b)^2 &= T^{-1}\sum_{t=2}^{T} w_t^2(\Delta P_t)^2 \\
&= T^{-1}\sum_{t=2}^{T}(\Delta P_t)^2 + T^{-1}\sum_{t=2}^{T}(w_t^2-1)(\Delta P_t)^2 \\
&= T^{-1}\sum_{t=2}^{T}(\Delta P_t)^2 + O_p(T^{-1/2}) \\
&\xrightarrow{w}_p \int_0^1 \sigma(r)^2 dr + \int_{\tau_{b1}}^{\tau_{b2}} \omega(r)^2 dr + \left\{\int_{\tau_{b1}}^{\tau_{b2}} e^{c(\tau_{b2}-s)(\tau_{b2}-\tau_{b1})^{-1}}\omega(s)dW_\eta(s)\right\}^2 .
\end{aligned}
$$

Hence,

$$
\begin{aligned}
S_{\bar{c}}^{*b}(\tau_1,\tau_2) &= \frac{\bar{c}^2(t_2-t_1)^{-2}\sum_{t=t_1+1}^{t_2}\left(\sum_{j=t}^{t_2}\{1+\bar{c}(t_2-t_1)^{-1}\}^{j-t}\Delta P_j^b\right)^2}{T^{-1}\sum_{t=2}^{T}(\Delta P_t^b)^2} \\
&\xrightarrow{w}_p \frac{\bar{c}^2(\tau_2-\tau_1)^{-2}\int_{\tau_1}^{\tau_2}\left\{\int_r^{\tau_2} e^{\bar{c}(s-r)(\tau_2-\tau_1)^{-1}}dK_0(s,\omega(\cdot),\sigma(\cdot),\tau_{b1},\tau_{b2})\right\}^2 dr}{\int_0^1\sigma(r)^2dr + \int_{\tau_{b1}}^{\tau_{b2}}\omega(r)^2dr + \left\{\int_{\tau_{b1}}^{\tau_{b2}} e^{c(\tau_{b2}-s)(\tau_{b2}-\tau_{b1})^{-1}}\omega(s)dW_\eta(s)\right\}^2} \\
&=: H_{0,\bar{c}}(\tau_1,\tau_2,\omega(\cdot),\sigma(\cdot),\tau_{b1},\tau_{b2}). \qquad \text{(A.6)}
\end{aligned}
$$

By the same arguments as made at the end of the proof of Theorem 1, it then follows from the fixed τ_1,τ_2 representation in (A.6) and the CMT that

$$
S_{\bar{c}}^{*b} \xrightarrow{w}_p \sup_{\tau_1\in[0,1-\pi]}\ \sup_{\tau_2\in[\tau_1+\pi,1]} \log H_{0,\bar{c}}(\tau_1,\tau_2,\omega(\cdot),\sigma(\cdot),\tau_{b1},\tau_{b2}).
$$

A.4 Allowing for a Drift in the Fundamental Price

As discussed in Remark 3.6, a drift in the fundamental price can be accounted for by modifying $S_{\bar{c}}^*$ through replacement of ΔP_t in both the numerator of (19) and in the variance estimate, $\hat{\sigma}^2$, by its de-meaned equivalent, $\Delta P_t - (T-1)^{-1}\sum_{t=2}^{T}\Delta P_t$. For this modified statistic, which we denote by $\bar{S}_{\bar{c}}^*$, it can be shown that the limiting behavior is the same as under Theorem 1 but with $K_c(r, \omega/\sigma, \tau_{b1}, \tau_{b2})$ of (21) replaced by

$$\begin{aligned}\bar{K}_c(r, \omega/\sigma, \tau_{b1}, \tau_{b2}) \quad := \quad & W_\varepsilon(r) - rW_\varepsilon(1) - \mathbb{I}(\tau_{b2} = 1) r \frac{\omega}{\sigma} \int_{\tau_{b1}}^{1} e^{c(1-s)(1-\tau_{b1})^{-1}} dW_\eta(s) \\ & + \mathbb{I}(\tau_{b1} \leq r \leq \tau_{b2}) \frac{\omega}{\sigma} \int_{\tau_{b1}}^{r} e^{c(r-s)(\tau_{b2}-\tau_{b1})^{-1}} dW_\eta(s). \end{aligned} \tag{A.7}$$

The corresponding modification to the $S_{\bar{c}}^{\dagger}$ statistic involves replacing ΔP_t with $\Delta P_t - (T-1)^{-1} \sum_{t=2}^{T} \Delta P_t$ in the numerator of (24), and replacing the variance estimate $\hat{\sigma}_m^2$ of (22) with $T^{-1} \sum_{t=2}^{T} \left\{ \Delta P_t^{\diamond} - (T-1)^{-1} \sum_{s=2}^{T} \Delta P_s^{\diamond} \right\}^2$, where $\Delta P_t^{\diamond} = \Delta P_t$ for all t except $t = \arg\max_{s \in [2,\ldots,T]} |\Delta P_s|$, in which case $\Delta P_t^{\diamond} = 0$. The limiting behavior of this variant, which we denote by $\bar{S}_{\bar{c}}^{\dagger}$, will be the same as under Corollary 2 but with $K_c(r, \omega/\sigma, \tau_{b1}, \tau_{b2})$ in $N_{c,\bar{c}}(\tau_1, \tau_2, \omega/\sigma, \tau_{b1}, \tau_{b2})$ of (25) replaced by $\bar{K}_c(r, \omega/\sigma, \tau_{b1}, \tau_{b2})$ of A.7.

Finite sample and asymptotic critical values for the $\bar{S}_{\bar{c}}^{*}$ and $\bar{S}_{\bar{c}}^{\dagger}$ tests are given in Table A.2, with the finite sample values reported for cases where the k largest absolute values of ΔP_t are removed when calculating $\bar{S}_{\bar{c}}^{\dagger}$.

Table A.2: Finite Sample and Asymptotic 10%, 5% and 1% Critical Values for $\bar{S}_4^{*}$ and $\bar{S}_4^{\dagger}$.

	10% Level				5% Level				1% Level			
T	100	200	400	∞	100	200	400	∞	100	200	400	∞
$\bar{S}_4^{*}$	8.358	8.630	8.824	8.993	8.490	8.762	8.938	9.112	8.744	8.986	9.182	9.309
$\bar{S}_4^{\dagger}$, $k=1$	8.440	8.679	8.852	8.993	8.568	8.807	8.967	9.112	8.838	9.036	9.209	9.309
$\bar{S}_4^{\dagger}$, $k=2$	8.506	8.718	8.873	8.993	8.641	8.842	8.990	9.112	8.908	9.078	9.232	9.309
$\bar{S}_4^{\dagger}$, $k=3$	8.569	8.755	8.893	8.993	8.702	8.879	9.010	9.112	8.972	9.112	9.249	9.309

Remark A.4.1. In the case of allowing for weakly dependent errors, adjustments to $\bar{S}_{\bar{c}}^{*}$ and $\bar{S}_{\bar{c}}^{\dagger}$ follow the same approach as discussed in section 6, but with $\hat{\lambda}^2$ of (28) based on $\Delta P_t - (T-1)^{-1} \sum_{t=2}^{T} \Delta P_t$ and $\Delta P_t^{\diamond} - (T-1)^{-1} \sum_{t=2}^{T} \Delta P_t^{\diamond}$, respectively, in place of ΔP_t. $\diamondsuit$

Remark A.4.2. The methods outlined in section A.2 to allow for unconditional heteroskedasticity can also be straightforwardly extended to cover the case where a non-zero drift term is allowed in the price series, P_t. Here, analogously to the results in the homoskedastic case, the $\bar{S}_{\bar{c}}^{*}$ and $\bar{S}_{\bar{c}}^{\dagger}$ statistics, based on the de-meaned data, will have limiting distributions of the form given in Theorem A.1 on replacing $K_c(r, \omega(\cdot), \sigma(\cdot), \tau_{b1}, \tau_{b2})$ with

$$\begin{aligned}\bar{K}_c(r, \omega(\cdot), \sigma(\cdot), \tau_{b1}, \tau_{b2}) \;\; := \;\; & \int_0^r \sigma(s) dW_\varepsilon(s) - r\int_0^1 \sigma(s) dW_\varepsilon(s) \\ & -\mathbb{I}(\tau_{b2} = 1) r \int_{\tau_{b1}}^1 e^{c(1-s)(1-\tau_{b1})^{-1}} \omega(s) dW_\eta(s) \\ & +\mathbb{I}(\tau_{b1} \leq r \leq \tau_{b2}) \int_{\tau_{b1}}^r e^{c(r-s)(\tau_{b2}-\tau_{b1})^{-1}} \omega(s) dW_\eta(s).\end{aligned}$$

Algorithm A.1 is also easily adapted to this case by replacing $S_{\bar{c}}^{\dagger}$ in Step 1 with $\bar{S}_{\bar{c}}^{\dagger}$, and replacing ΔP_t^b in $S_{\bar{c}}^{*b}(\tau_1, \tau_2)$ of (A.2) with the de-meaned bootstrap data $\Delta P_t^b - (T-1)^{-1}\sum_{t=2}^T \Delta P_t^b$. For the bootstrap statistics based on the de-meaned bootstrap data, the asymptotic null distribution coincides with the limiting null distribution of the $\bar{S}_{\bar{c}}^{\dagger}$ statistic. Bootstrap validity therefore also holds in this case. $\diamondsuit$

A.5 Time-Varying AR(1): Simulation DGP and Results

We consider three TVAR(1) DGPs, the first where the price series P_t begins as a unit root process until time $t = \lfloor \tau_1 T \rfloor$ before a bubble occurs running until $t = \lfloor \tau_2 T \rfloor$, after which point the price series reverts to a unit root process until the end of the sample, i.e.

$$P_t = \begin{cases} P_{t-1} + \varepsilon_t & t = 1, \dots, \lfloor \tau_1 T \rfloor \\ \phi_1 P_{t-1} + \varepsilon_t & t = \lfloor \tau_1 T \rfloor + 1, \dots, \lfloor \tau_2 T \rfloor \\ P_{t-1} + \varepsilon_t & t = \lfloor \tau_2 T \rfloor + 1, \dots, T. \end{cases}$$

The second DGP considers the case where the price series P_t again begins as a unit root process followed by a bubble regime, but then subsequently follows a stationary collapse regime from time $\lfloor \tau_2 T \rfloor + 1, ..., \lfloor \tau_3 T \rfloor$, before the series reverts to a unit root process from $t = \lfloor \tau_3 T \rfloor + 1$ until the end of the sample, i.e.

$$P_t = \begin{cases} P_{t-1} + \varepsilon_t & t = 1, \ldots, \lfloor \tau_1 T \rfloor \\ \phi_1 P_{t-1} + \varepsilon_t & t = \lfloor \tau_1 T \rfloor + 1, \ldots, \lfloor \tau_2 T \rfloor \\ \phi_2 P_{t-1} + \varepsilon_t & t = \lfloor \tau_2 T \rfloor + 1, \ldots, \lfloor \tau_3 T \rfloor \\ P_{t-1} + \varepsilon_t & t = \lfloor \tau_3 T \rfloor + 1, \ldots, T. \end{cases}$$

Finally, we consider a DGP where the price series P_t begins as a unit root process followed by a bubble regime, with the price series then collapsing to its pre-bubble level, before reverting to unit root behavior thereafter, i.e.

$$P_t = \begin{cases} P_{t-1} + \varepsilon_t & t = 1, \ldots, \lfloor \tau_1 T \rfloor \\ \phi_1 P_{t-1} + \varepsilon_t & t = \lfloor \tau_1 T \rfloor + 1, \ldots, \lfloor \tau_2 T \rfloor \\ P_{\lfloor \tau_1 T \rfloor} + \varepsilon_t & t = \lfloor \tau_2 T \rfloor + 1 \\ P_{t-1} + \varepsilon_t & t = \lfloor \tau_2 T \rfloor + 2, \ldots, T. \end{cases}$$

We set $\tau_1 = 0.3$, $\tau_2 = 0.5$ and $\tau_3 = 0.7$. We generate the innovations as $\varepsilon_t \sim NIID(0,1)$ and set $\phi_1 = 1 + c^*/T$, and for the stationary collapse model set $\phi_2 = 1 - c^*/T$. We examine the power of the tests for a grid of values of $c^* \in (0, 30]$. Given that the best overall performance for the $S^*_{\bar{c}}$ and $S^\dagger_{\bar{c}}$ tests in the previous scenarios was given by $\bar{c} = 4$ we report results for the S^*_4, $S^\dagger_4$ and $GSADF$ tests in Figure A.1.

Figure A.1: Finite sample power of nominal 5% tests, AR DGP, $T = 200$,

$\tau_1 = 0.3$, $\tau_2 = 0.5$, $\tau_3 = 0.7$.

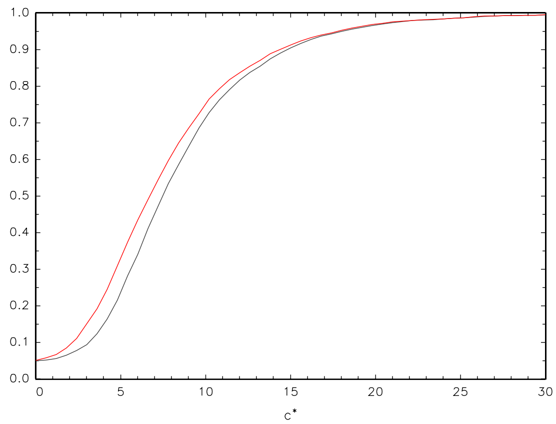

(a) No crash, $GSADF$ and S_4^* tests

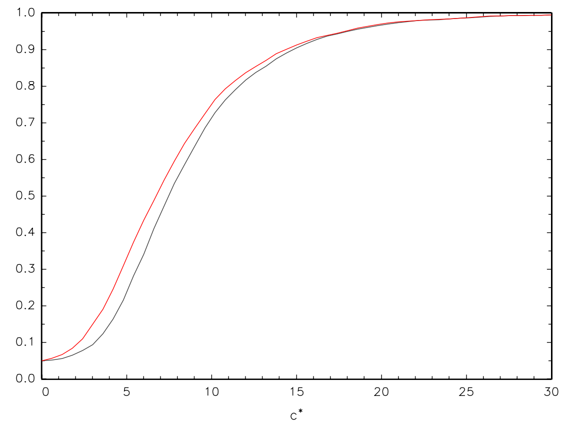

(b) No crash, $GSADF$ and $S_4^\dagger$ tests

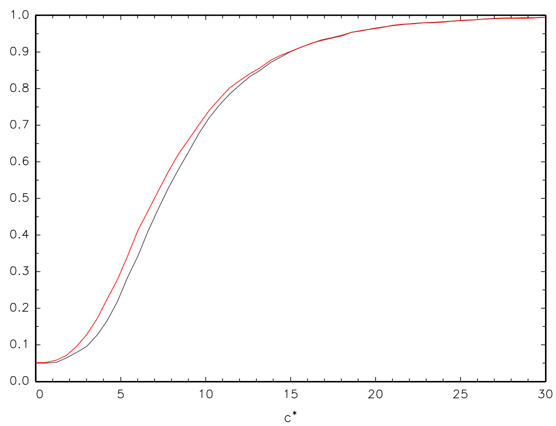

(c) Stationary crash, $GSADF$ and S_4^* tests

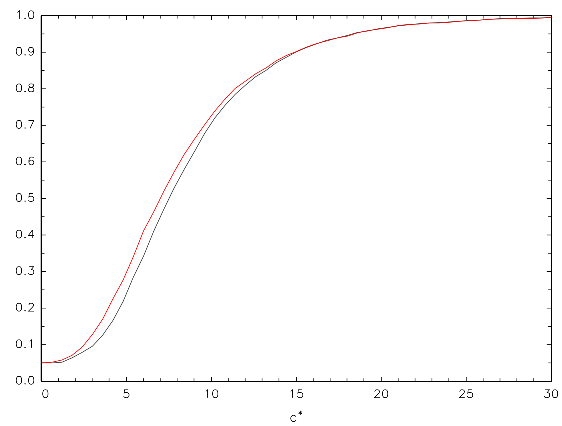

(d) Stationary crash, $GSADF$ and $S_4^\dagger$ tests

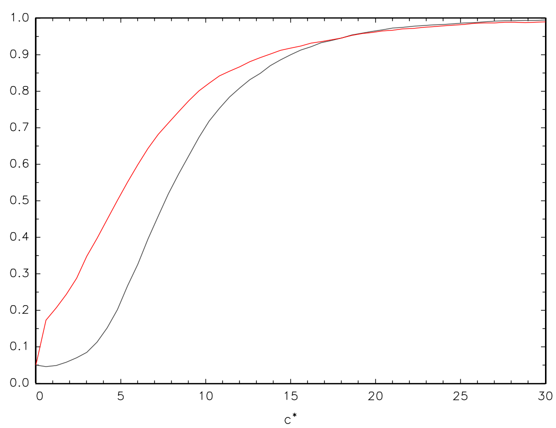

(e) Instantaneous crash, $GSADF$ and S_4^* tests

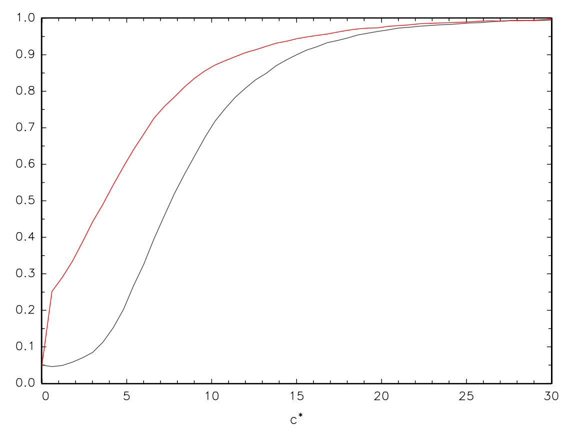

(f) Instantaneous crash, $GSADF$ and $S_4^\dagger$ tests

$GSADF$: —— , $S_4^*, S_4^\dagger$: ——

A.6 Graphs of Empirical Data Series

Figure A.2: Graphs of Empirical Series

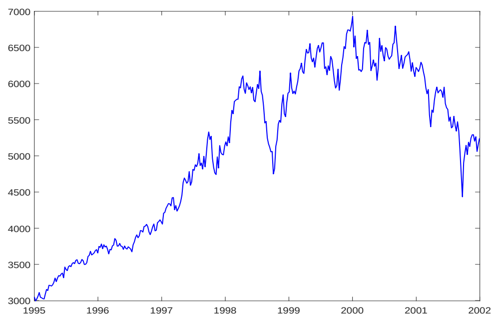

(a) FTSE

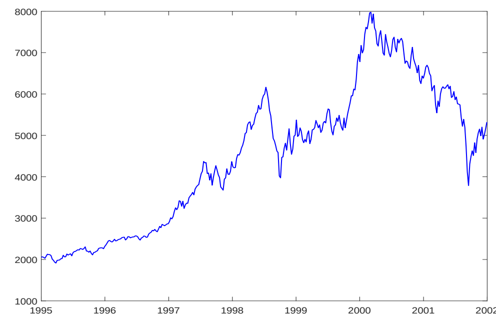

(b) DAX

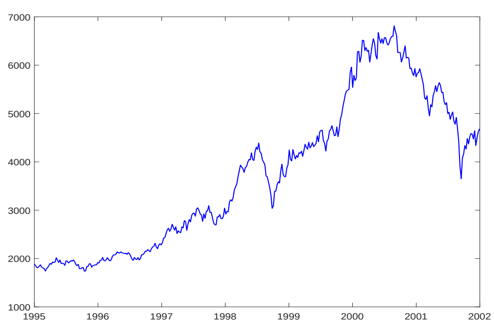

(c) CAC40

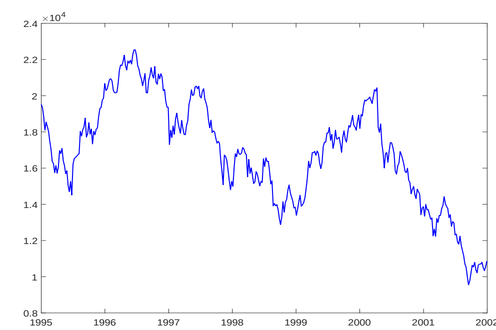

(d) Nikkei

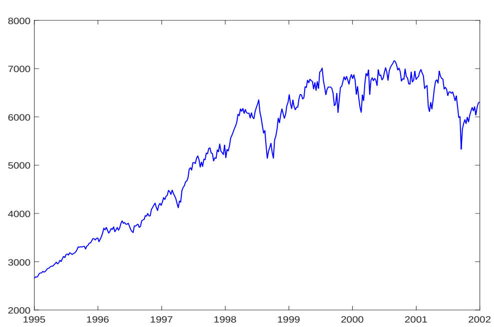

(e) NYSE Composite

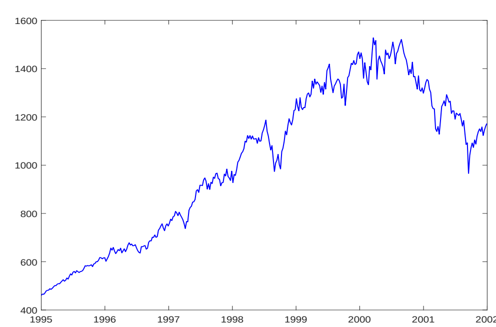

(f) S&P500

Figure A.2: Continued ...

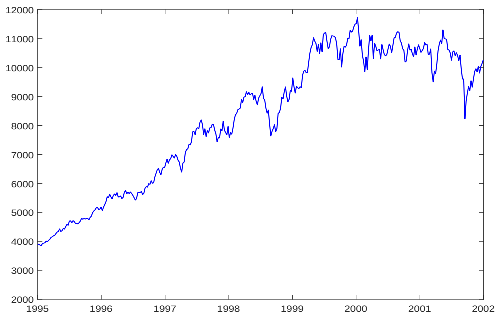

(g) Dow Jones Industrial Average

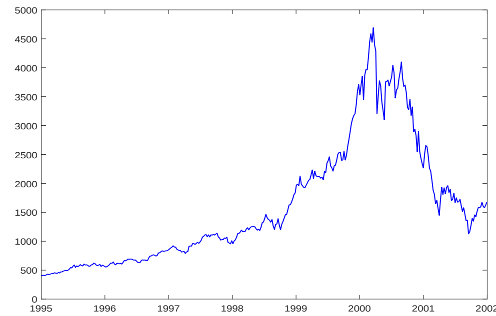

(h) NASDAQ100

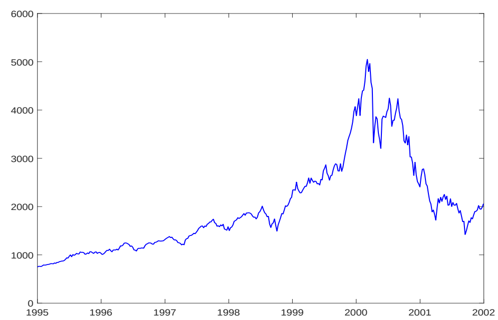

(i) NASDAQ Composite

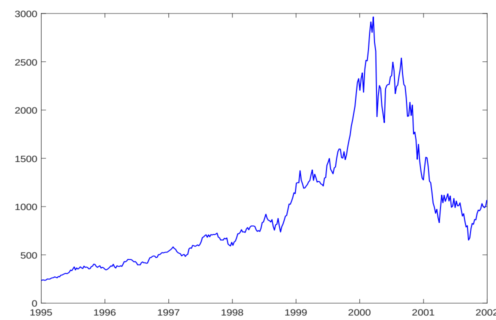

(j) NASDAQ Computer

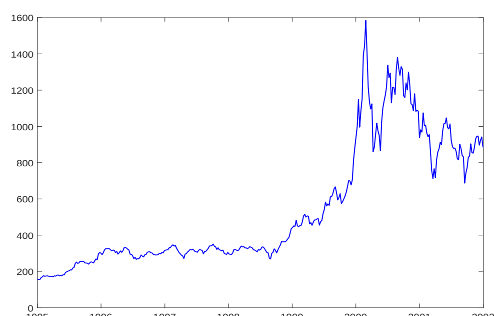

(k) NASDAQ Biotech

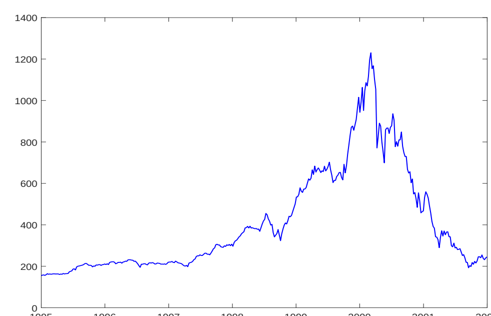

(l) NASDAQ Telecomms

Additional References

Calvo-Gonzalez, O., Shankar, R. and Trezzi, R. (2010). Are commodity prices more volatile now? World Bank Policy Research Working Paper 5460.

Harvey, D.I., Leybourne, S.J., Sollis, R. and Taylor, A.M.R. (2016). Tests for explosive financial bubbles in the presence of non-stationary volatility. Journal of Empirical Finance 38, 548-574.

McMillan, D.G. and Wohar, M.E. (2011). Structural breaks in volatility: the case of UK sector returns. Applied Financial Economics 21, 578-595.

Vivian, A. and Wohar, M.E. (2012). Commodity volatility breaks. Journal of International Financial Markets, Institutions and Money 22, 395-422.

Zivot, E., & Andrews, D.W.K. (1992). Further evidence on the great crash, the oil-price shock, and the unit-root hypothesis. Journal of Business and Economic Statistics 10, 251–270.